Long-Term Trends in Gas-Particle Partitioning of Reduced Reactive Nitrogen Species, as Analyzed by Annular Denuders and Ion Chromatography

by

Jared Asher William Schlenker

Undergraduate Honors Thesis in Department of Chemistry

University of Colorado at Boulder

Defense Date: 20 October 2022

Advisor: Eleanor Browne, Department of Chemistry

Committee:

Boswell Wing, Department of Geological Sciences

Eleanor Browne, Department of Chemistry

Robert Parson, Department of Chemistry

Abstract

Reduced reactive nitrogen species, which primarily consist of ammonia and low-mass amines, occur in the gas-phase and the particle-phase of the atmosphere. Despite being present at trace concentrations, these species can have severe effects on eutrophication, biodiversity, human pulmonary and cardiac health, and deposition. Long-term sampling of these species is infrequent, and such sampling that has taken place is focused around agricultural sources rather than urban environments. A greater understanding of the gas-particle partitioning of these species elucidates our understanding of the roles they play in the aforementioned environmental effects.

I adapted the EPA's procedure for the sampling of ambient air using annular denuders and performed troubleshooting techniques on an ion chromatograph to develop a method to collect and analyze reduced nitrogen species; with this method, phases can be examined separately, thus allowing for a greater understanding of the magnitude of each risk associated with the gas and particle-phases rather than conflating the total concentration together. Method development is a crucial step in initiating long-term sampling, because consistency is the foundation of accuracy. I began preliminary ambient sampling with a focus on ensuring the procedure works and exploring potential trends.

While further sampling over the course of years will be necessary to confirm trends, some trends are beginning to emerge: gas-phase ammonia is present in higher concentrations when the average temperature is greater. The total concentration and the ratio of gas-to-particle concentrations are still being considered, as are these apparent trends. For the future, focus should be directed towards identifying the dominant source of analyte in the second annular denuder, observing effects of different filters, refining the gradient method, and considering the maximum collectable concentration on the denuders and filter.

Acknowledgements

There were quite a number of people who were instrumental to my success throughout this project, and I would like to provide them with thanks for their work, assistance, and insight.

First, I would like to thank Dr Eleanor Browne for providing me with the opportunity to work in your lab for the last 18 months. You have spent numerous hours meeting and brainstorming with me, as well as providing edits and comments on my presentations and writings. Your breadth and depth of atmospheric chemistry is truly astounding, and has been extremely helpful throughout my work. You have always been incredibly patient and kind and I thank you for this.

Second, I would like to thank McKenzie Larson for training me on instrumentation as well as many general scientific practices. You pushed me to think independently and out-of-the-box when it comes to problem-solving, while still being available when I need a helping hand.

Further, I would like to thank the rest of the Browne group for the feedback on writing techniques, presentation skills, and figure creation. With your help, I have been constantly learning in the lab and growing as a scientist.

Next, thank you to Dr Robert Parson and Dr Boswell Wing for agreeing to be on my honors committee. The feedback you provide is extremely useful, especially from scientific minds outside of the specific field of atmospheric chemistry. I also appreciate your understanding and patience through technical difficulties.

Thank you to my family for your unwavering support through good times and hard times. While none of you consider yourself scientists, I am thankful that you were always willing to listen to my long ramblings about my research. Whether I needed a new perspective, a proofreader, or a shoulder to cry on, I could always count on you all being there for me.

I am very grateful to have received grant funding from the Undergraduate Research Opportunity Program (UROP) in the summer of 2022. This allowed me to continue my work and pursue my passion during the summer, unhindered by financial need.

Finally, I want to thank all of my high school teachers and college professors. Your job is one of the hardest and one of the most valuable. You have all helped shape me into the person I am today, and you continue to do so every day with countless more students.

Table of Contents

List of Figures

1. Introduction

Beginning in the mid-20th century, changes in agricultural practices such as new developments in animal husbandry and expansion of farmland combined with increasing fossil fuel combustion, resulted in rapid and significant modifications to the reactive nitrogen cycle.[1] Since the 1980s, anthropogenic emissions of reactive nitrogen species (N_r) have exceeded that of natural terrestrial ecosystems.[1] Additionally, there is a strong linear correlation between the growths in N_r emissions and human population; when the population grows by 1 billion, the annual anthropogenic emissions of N_r increases by 25 teragrams, which is a growth of around 5%.[1]

N_r are all forms of nitrogen that are chemically, biologically, or radiatively active; for comparison, nitrogen gas (N_2) makes up ~78% of the atmosphere, but this form of nitrogen is chemically inert at normal temperatures and pressures. N_r species can be broadly categorized into oxidized and reduced nitrogen. Oxidized nitrogen includes NO_x (nitric oxide and nitrogen dioxide). Sources of NO_x consist of a variety of high-temperature processes such as vehicles combusting fossil fuels, lightning, electric power generation, industrial boilers, and cement kilns.[2,3] In the last few decades, regulations were put in place in the United States, China, and Europe to decrease the atmospheric concentration of NO_x due to its effects on fine particles and ground level ozone.[4,5] This legislation was largely successful in the United States; measurements made over three year periods at the CASTNET sites in the eastern United States show that atmospheric NO_x concentrations from 2014 to 2016 were 57% less than from 1990 to 1992.[6] This decrease is attributed to limitations placed by the Clean Air Act Amendments.[6] The largest contributor to reduced N_r is NH_3 and ammonium. In the United States, more than 80% of NH_3 emissions originate from the agricultural sector, specifically livestock waste and nitrogen-based fertilizer.[2,6] The NH_3 emissions from animal waste are highly-dependent on atmospheric physical state; when temperature varied from 5℃ to 25℃, the emission rate from this source increased by a factor of nine.[7] There are also natural sources such as forest fires and decomposition of waste in non-agricultural soil.[8,9] In contrast to the decreasing NO_x emission trends described above, NH_3 emissions increased by 72% between 1980 and 2018.[10] As a result of these emission changes, the composition of N_r is shifting from being previously dominated by oxidized nitrogen to one where reduced nitrogen is becoming increasingly important.[2] Furthermore, NH_3 emissions are largely unregulated, so this domination is likely to continue into the foreseeable future.[2] Other than the Euro VI standard, which limits NH_3 emissions on heavy-duty diesel vehicles, there are no NH_3 regulations worldwide (a recent change is that, in June of 2022, lawmakers in the Netherlands voted to decrease national NH_3 emissions by 50% with a focus on agricultural sources — this was met with protests).[11,12] To reiterate this point, four representative concentration pathway (RCP) anthropogenic emission scenarios, which come from integrated assessment models, were constructed by adjusting socioeconomic and technological parameters. All RCP scenarios found NH_3 emissions would increase by 19 to 50% in the United States and by 26 to 57% globally by the year 2050.[13] NH_3, once emitted, can form NH_4^+ (ammonium) aerosols by reacting with acids; generally, NH_3 reacts with sulfuric acid to form ammonium sulfate or with nitric acid to form ammonium nitrate.[2]

An interesting consideration is the expected transport distance for reactive nitrogen in the atmosphere. Gaseous nitrogen — NH_3 — has an atmospheric lifetime on the order of hours, because, once emitted, it rapidly deposits to surfaces or forms particulate matter.[4] Particulate matter is mixture of solid and liquid particles in the air and it is generally classified for regulatory purposes as either PM_{10} or $PM_{2.5}$ which are inhalable coarse particles and fine

particles respectively; PM_{10} is less than 10 micrometers in diameter and $PM_{2.5}$ is less than 2.5 micrometers in diameter.[14] $PM_{2.5}$, specifically, is of interest because of the component breakdown of each of these types of particulate matter: PM_{10} is mostly composed of soil, dust, and bioaerosols whereas $PM_{2.5}$ contains much more ammonium salts.[15] Beyond the component breakdown, $PM_{2.5}$ is more harmful to human health, because it penetrates deeper into the lungs; the World Health Organization says that $PM_{2.5}$ exposure is linked with the greatest proportion of negative health effects from air pollution.[16] $PM_{2.5}$ has a lifetime of over a week, allowing the NH_3 to travel significantly farther from the source (several hundred kilometers) before being deposited into what might otherwise be unperturbed ecosystems.[11,17,18] Aerosols worsen air quality and visibility and also alter the atmospheric radiative balance, which is related to earth's incoming and outgoing energy.[19] Large concentrations of atmospheric particulate matter leads to increased risk of pulmonary and cardiac disorders; this is especially true for $PM_{2.5}$.[18] This interaction that forms particulate matter is especially concerning in urban environments, because recent research has found that NH_3 emissions from vehicles is vastly underestimated. The first source of NH_3 in vehicles is that it is an unintended result of decreasing NO_x in vehicle exhaust.[11,20] For a long time, there was little consensus on how large this byproduct was. However, a more recent second source of NH_3 in vehicles is called NH_3 slip, which is caused by the urea used for limiting NO_x in three-way catalytic converters.[11] Excessive use of urea, low temperatures, and catalyst degradation can all cause accidental NH_3 emissions.[11] More recent studies that account for the latter of these two sources have found that NH_3 from vehicle exhaust is roughly twice national inventories.[20] Urban areas, which already have high concentrations of atmospheric NO_x, are especially at risk of $PM_{2.5}$ formation given that NH_3 emissions from vehicles are significantly higher than previously thought.

Reactive nitrogen also plays a vital role in many environmental phenomena, including nitrogen deposition.[21] Deposition is a process by which reactive nitrogen species transition from the atmosphere to the biosphere either through dry deposition, or through scavenging by precipitation, known as wet deposition; gasses and particles can each undergo both of these types of deposition. Nitrogen deposition is one reason motivating the study of long-term N_r sampling, due to the role nitrogen serves in all life. Nitrogen is an essential element for ecosystems, and is often a limiting element, so increased deposition could lead to improved efficiency and productivity in ecosystems.[22] However, growing N_r emissions leads to excessive nitrogen deposition, oftentimes beyond the local critical load.[23] Critical loads are thresholds that quantify the level at which a given pollutant will begin to have harmful effects, as determined by dose-response measurements.[23] In large quantities, N_r deposition poses threats to various environmental areas, including water, soil, and plantlife. The most common effect of excess nitrogen in water is eutrophication and acidification.[24] Furthermore, plants may become more susceptible to drought and become less resistant to pests and pathogens.[17,22]

Another method by which particulate matter can form is when amines, another form of reduced nitrogen, react with nitric acid and sulfuric acid. In aerosols, amines tend to be present in trace amounts (in some Colorado national parks, this concentration was between 0.02 to 0.09 $\mu g/m^3$).[25] Even so, they have received a lot of attention recently due to their participation and acceleration of new particle formation events.[26] Amine emissions are estimated to have grown significantly over the last 200 years, mainly from animal husbandry. Other sources include internal combustion engines and biomass burning.[27] More recently, carbon capture and storage facilities have become another source; amines are used for the reversible collection of atmospheric carbon dioxide.[27] At this time, anthropogenic sources of amines have overtaken

natural sources. Methylamine, dimethylamine, and trimethylamine are the most common amines found in the atmosphere.[27] These low-mass amines exhibit high solubility in water and are stronger bases than NH_3.[28] The first of these properties means that amines are likely to enter the biosphere via wet deposition and, therefore, not travel very far from the source.[25] The second of these properties means that acid-base interactions with nitric acid and sulfuric acid are likely to occur with amines even in the presence of NH_3.[28] Other considerations, when studying amines, include the low atmospheric concentrations which make them difficult to quantify as well as the similar retention times among low-mass amines which makes them difficult to separate. Despite these analytical challenges, it is important to consider amines, because of the ways they can alter NH_3 partitioning through their displacement in NH_4^+ salts.[27,29] Amines also help facilitate new particle formation (NPF) events; by considering trends in amine concentrations along with amine sources, predictions of NPF events can be strengthened.[27,29]

Currently, the EPA's NH_3 monitoring network is largely focused on agricultural sources; as such, this network does not have any urban monitoring sites.[20] It is crucial to improve our understanding of NH_3 emission inventories in order to more-fully grasp the role NH_3 plays in various environmental interactions. Currently, NH_3 measurements are a high-priority for long-term sampling since it is the only inorganic aerosol precursor which has a projected increase in emission over the next century and long-term measurements are scarce.[30,31] To address the need for improved understanding of reduced reactive nitrogen species in the atmosphere, I established a method for conducting long-term sampling in Boulder, Colorado based on the EPA's annular denuder set-up. I began with troubleshooting of a cation chromatography instrument such that it could be utilized to create calibration curves for each of the analytes of interest. Various operational techniques were adjusted to improve resolution while decreasing the time needed to analyze. Then, a sampling apparatus was constructed that included two coated annular denuders and a nylon filter which, by pumping ambient air through them, collected reduced nitrogen species from the gas and particle-phases. The extract from the denuders and filter were analyzed using the ion chromatograph and the concentrations of each analyte was determined using the calibration curves. Within this project, I performed this sampling process for several months to obtain preliminary results and to fine-tune the process, so that future researchers can continue sampling utilizing the methods developed here. The end results should help answer questions about the concentration of reduced nitrogen species per unit volume of ambient air, the phase partitioning of N_r in the gas and particle-phases, the seasonal effects on these concentrations, and the sources of these species in the Boulder area.

2. Methods

2.1. Ion Chromatography

Ion chromatography is a technique that separates analytes based on their affinity to a macroporous divinylbenzene/ethylvinylbenzene polymeric resin.[31] The different species in the sample have varying affinities for the resin and, therefore, diffuse into the stationary phase at different rates.[34] While some ions have a strong affinity for the stationary phase, others are much more strongly attracted to the eluent. These different affinities cause species to separate while in the column and elute at different times.[34] In the set-up utilized in this experiment, the eluent was 8 millimolar (mM) methanesulfonic acid (MSA). The detector at the end of the instrument monitors the electric conductivity as a function of time in units of micro Siemens (μS). The conductivity will greatly increase from the background at specific times during the elution, producing peaks on the chromatogram, where each peak corresponds to a different species in the sample. The particular ion chromatograph (IC) utilized in this procedure is a cation IC, which has a negatively charged stationary phase and works to separate positively charged species; anion chromatography, on the other hand, measures negatively charged species. Figure 1 shows one cell of the ion chromatograph, which contains the columns, suppressor, and detector.

2.1.1. Six-Port Valve

When using the IC, between 0.1 and 0.5 mL of a sample is injected into the six-port valve and is carried through the columns by the mobile phase. The six-port valve connects the injection port, the column, the waste, and a sample loop. The six-port valve has two configurations: inject and load. In inject mode, samples from the injection port enter into the sample loop. The sample loop is a specific length to ensure the same volume of sample is run through the column in each run; any excess sample added is sent directly to waste. The sample loop in this set-up holds 10 μL of sample. During this time, eluent goes through the column. In load mode, the connections of the six-port valve rotate causing the eluent to flow through the sample loop and then towards the columns. At the same time, the injection port is sent to waste, so no other sample can be added until the run completes.[34]

2.1.2. Guard and Analytical Columns

In load mode, the sample travels from the loop into the guard column prior to the analytical column. The purpose of the guard column is to remove larger particles and impurities before they can reach, and damage, the analytical column. In this way, the lifetime of the analytical column is prolonged. The sample travels from the guard column to the analytical column, carried by the mobile phase. The guard column has a 2 mm diameter and a 50 mm length. The analytical column has a 2 mm diameter and 250 mm length. The analytical columns contain a super macroporous resin containing carboxylic acid groups, which serves as the stationary phase.[32] The fact that the resin is macroporous allows the eluent to flow through unhindered. The guard column is packed with a microporous polymeric resin which is of a lower capacity, which means it cannot be used for separation on its own.[32] The mobile phase used is 8 millimolar (mM) MSA in nanopure water (also referred to as milli-Q). The mobile phase is pumped through the system at a flow rate of 0.20 mL/min.

2.1.3. Suppressor and Detector

Next, there is a suppressor after the columns and before the detector. The suppressor decreases the conductivity of the background eluent by displacing hydronium ions, which are

highly conductive, into the regenerant chamber; simultaneously, the suppressor increases the conductivity of the analytes by forming a salt, which has higher conductivity than partially ionized acids.[34,35] Suppression is necessary for being able to detect analytes, which have a lower conductivity than the eluent without suppression.[34] The suppressor also contains a back-pressure line that reduces any bubbles in the tubing, which is necessary because bubbles cause uneven flow of analytes and, therefore, broaden peaks.

Finally, there is the detector; as stated previously, the detector measures the conductivity as a function of time and the resulting chromatogram has peaks on it that each correspond to a different analyte. The retention time of each compound should remain consistent between sample runs as long as the operating characteristics — such as phases, the column, and temperature — are not changed. In other words, regardless of how complicated the matrix is, a given compound should always elute at the same time. Additionally, the area of the peak will be proportional to the analyte concentration. For this project, the version 8 of the Igor software (Wavementrics) was used to take the integral by using multi-peak fitting with assumed Gaussian curves.

2.1.4. Baseline Correction

To analyze the resulting chromatograms, the regions of each peak must be separated from the background. Correcting for the baseline must be done or the peak areas found using Igor will be over-estimates. On some early chromatograms, the background maintained at 0 μS before, after, and in between the peaks. However, later chromatograms exhibited "water dip" which adjusted the baseline from a constant conductivity of 0 μS. The "water dip" region is a drop in the signal that results when water enters the detector; it occurs because the conductivity of the water is less than the suppressed signal of the eluent.[36] Theoretically, the water dip negative peak should return to zero signal (the starting signal of the trial), but it never did in these trials. It likely started to rise up again, but this happened around the same time that the analytes started to reach the detector. For this reason of overlap, the baseline cannot simply be set at the lowest part of the water dip region. Additionally, the background conductivity after the analytes eluted was often higher than before. This means that the baseline is non-constant and, in fact, increasing over time.

To perform baseline correction, the region before the peaks of the analytes was located as well as the region after they had all eluted. Before the peaks, this region was identified as a kink in the signal to differentiate the rise of the water dip phenomenon from the peaks of the analytes. After the peaks, this region was identified as where the signal flattened out again. A ten-point-average was taken at each of these two identified points and the baseline was set to the linear increase from the earlier average to the later average. The conductivities predicted by this line were subtracted from the conductivities collected by the detector to find the baseline-corrected-signal at any given time. This subtraction was only done for the area of the chromatogram between the two regions chosen; the rest were set to zero, since the signal there is not of interest for this project. Figure 2 depicts this entire process, starting with the original chromatogram followed by the chromatogram with the baseline added, and finally showing the new chromatogram with the linear baseline subtracted from the collected signal.

The peak areas then have to be determined by fitting each peak to a Gaussian curve and taking the integral. Figure 3 and Figure 4 provide examples of this peak fitting; Figure 3 is a relatively simple system with only two compounds whereas Figure 4 contains more compounds. When several samples with different known analyte concentrations are analyzed, a calibration curve can be constructed for each compound. Each calibration curve depicts the linear

relationship between concentration and peak area. When a sample containing that compound in unknown concentration is run through the IC, the peak area can be plugged into the calibration curve equation to calculate the concentration of that compound. Errors in the determined concentration come from the intrinsic error in using a calibration curve and the error in the glassware used to measure the volume of the solvent.

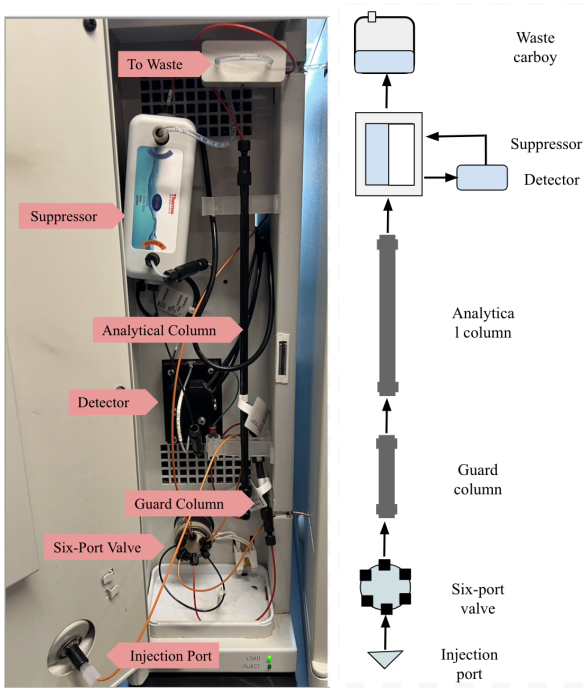

Figure 1. One cell of the ion chromatograph. This cell contains the pathway that injected samples follow as they travel through the instrument to be separated. The path, in order, is injection port, six-port valve, guard column, analytical column, suppressor, detector, suppressor again, and waste.

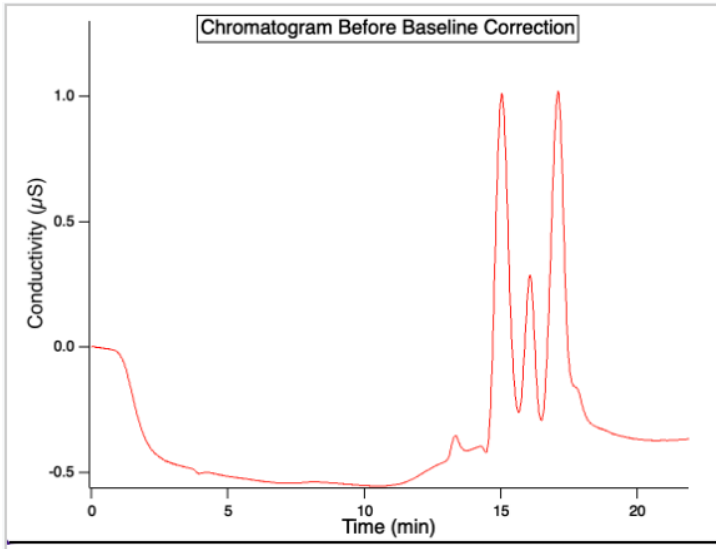
Chromatogram Before Baseline Correction
Conductivity (μS)
1.0
0.5
0.0
-0.5
0
5
10
15
20
Time (min)

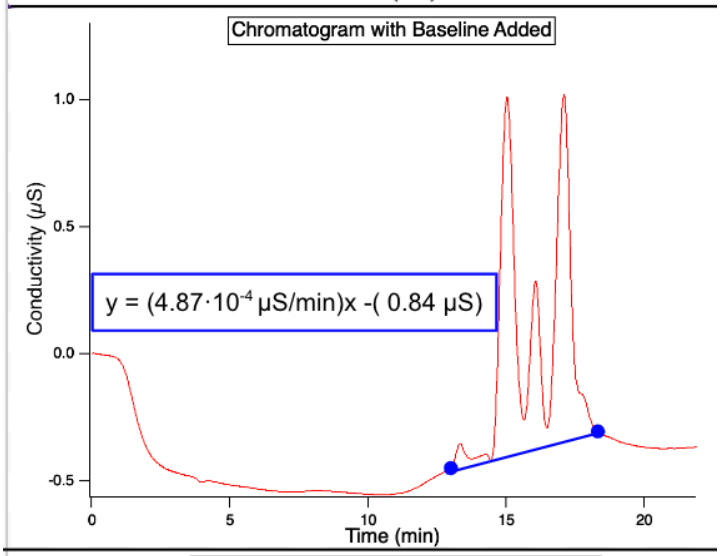
Chromatogram with Baseline Added
Conductivity (μS)
y = (4.87·10-4 μS/min)x -(0.84 μS)
1.0
0.5
0.0
-0.5
0
5
10
15
20
Time (min)

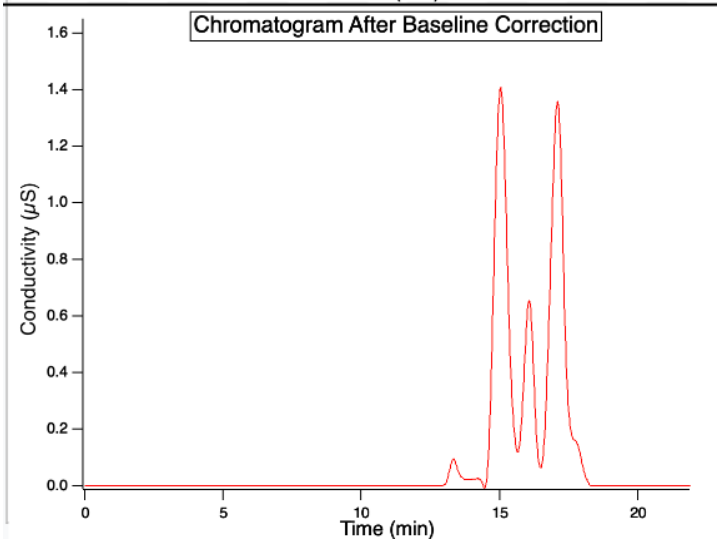
Chromatogram After Baseline Correction
Conductivity (μS)
1.6
1.4
1.2
1.0
0.8
0.6
0.4
0.2
0.0
0
5
10
15
20
Time (min)

Figure 2. A chromatogram of 1.4 mg/L ammonium, 0.4 mg/L methylamine, and 1.4 mg/L ethylamine. The three figures show the original chromatogram, the process of baseline correction, and the resulting chromatogram after the baseline is corrected.

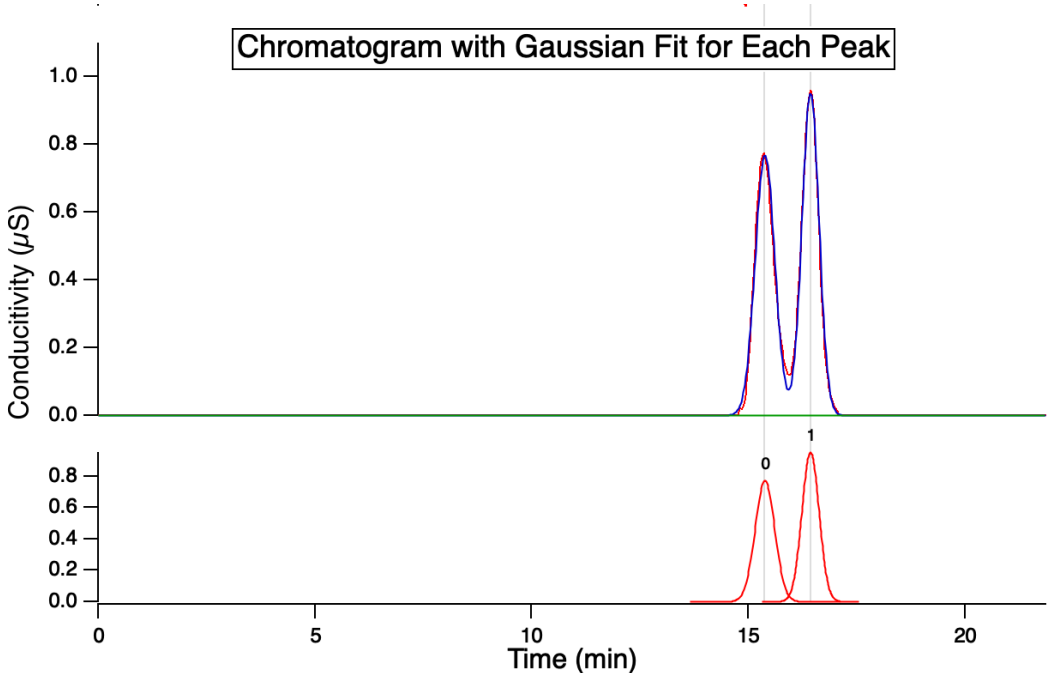

Peak	Location		Amplitude		Area		Width	
0	15.3820	± 0.0007	0.769	± 0.002	0.433_4	$\pm 0.001_2$	0.318_0	$\pm 0.001_0$
1	16.4340	± 0.0005	0.951	± 0.002	0.468_2	$\pm 0.001_1$	0.2779	± 0.0008

Figure 3. This top graph is the chromatogram for a mixture of 0.6 mg/L ammonium and 0.6 mg/L methylamine. The second graph includes red curves which are Gaussian fits for each of the peaks on the first graph. The baseline correction process described in Figure 2 has been done, so the only peaks present correspond to ammonium (Peak 0) and methylamine (Peak 1). The table includes the specific time, height, and amplitude of each peak.

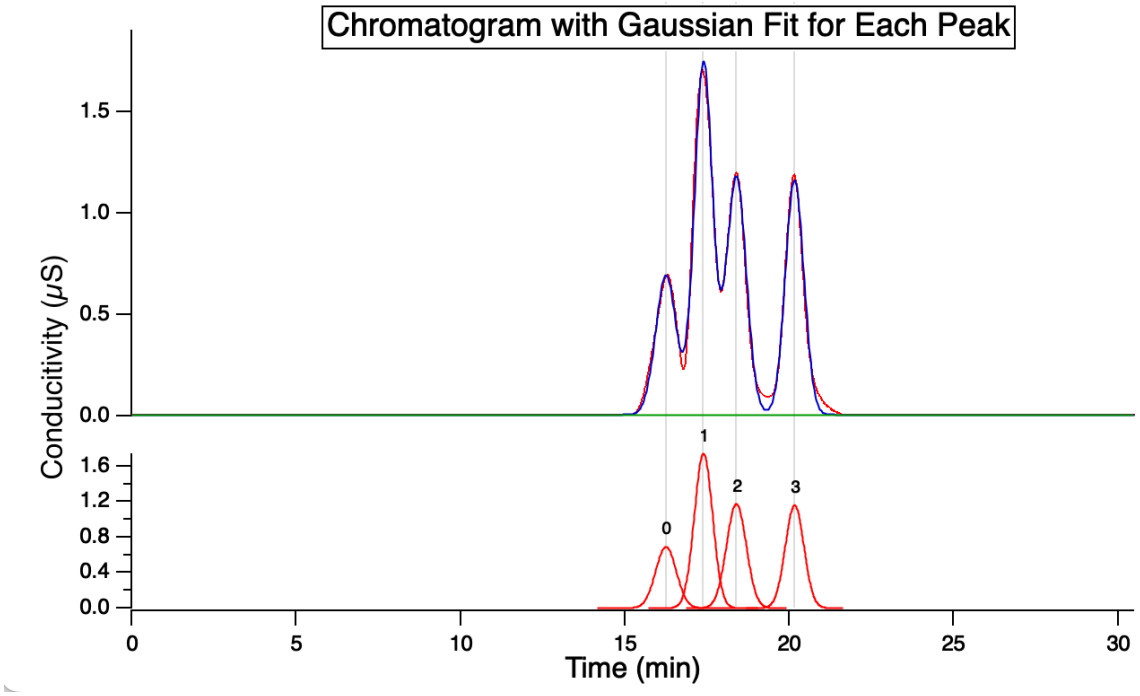

Peak	Location		Amplitude		Area		Width	
0	16.248	± 0.002	0.689	± 0.004	0.539	± 0.003	0.442	± 0.003
1	17.3890	± 0.0009	1.741	± 0.004	1.202	± 0.004	0.389_6	$\pm 0.001_4$
2	18.389_0	$\pm 0.001_3$	1.174	± 0.004	0.882	± 0.004	0.424	± 0.002
3	20.161_0	$\pm 0.001_1$	1.159	± 0.004	0.814	± 0.003	0.396_3	$\pm 0.001_5$

Figure 4. This top graph is the chromatogram for a mixture of 1.0 mg/L of each of ammonium, sodium, potassium, and methylamine. The second graph includes red curves which are Gaussian fits for each of the peaks on the first graph. Unlike Figure 2, the second graph has the analyte peaks overlapping, but they are still able to be separated with the Igor software

2.2. Ion Chromatograph Troubleshooting

The instrument utilized is older and has a tendency to behave inconsistently at times. As such, a considerable amount of time was spent learning these tendencies and troubleshooting the instrument. As a starting place, I observed the tendency for drift across days and even over the course of the same day. Two solutions of ammonium sulfate — one with a concentration of 1.0 mM and the other with a concentration of 2.0 mM — were run three times for several days over the course of two weeks. From one day to the next, the peak area on the chromatogram had a variability of up to 8.5% of the total area, which was enough to cause concern. While the specific areas would vary, the slopes of the preliminary calibration curves for each day were similar. One example of a chromatogram, specifically a 1.0 mM sample of NH_4^+, is shown in Figure 5. In Figure 6, four calibration curves including 1.0 mM and 2.0 mM ammonium are shown where each one varies based on the day the trials were done; Figure 7 has all of this data placed on one curve along with several trials of 1.5 mM ammonium.

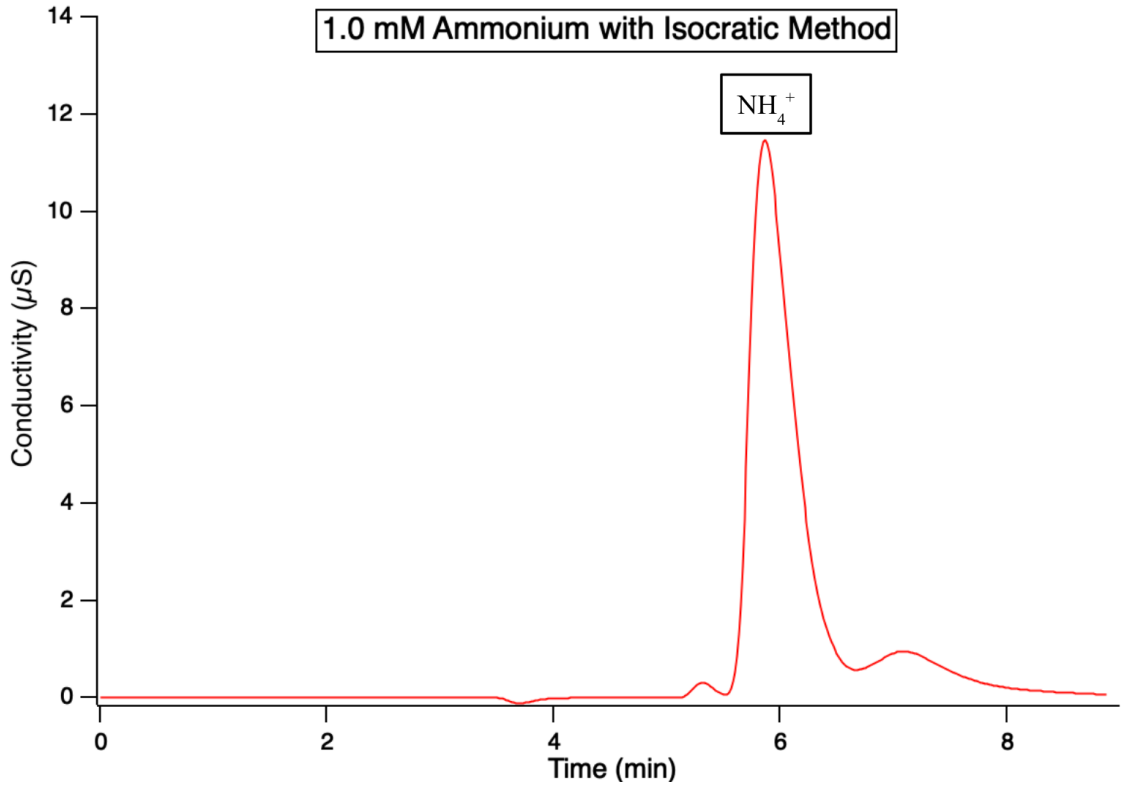

Figure 5. A chromatogram of 1.0 mM ammonium (0.5 mM ammonium sulfate) made using the isocratic method that has the mobile phase of 8.0 mM MSA run for 9 minutes.

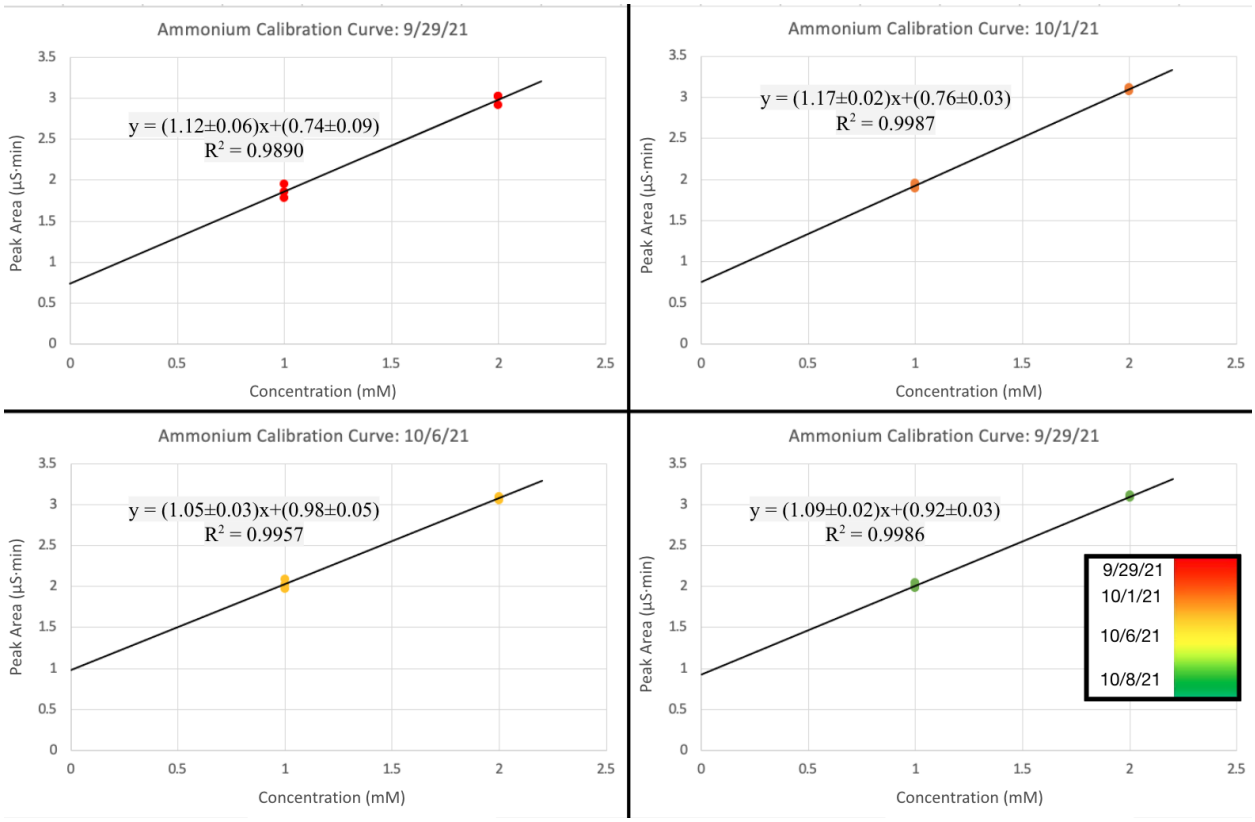

Figure 6. Four calibration curves for ammonium in the range of 1.0 mM to 2.0 mM. Each was made on separate days to examine the instrumental drift in the ion chromatograph.

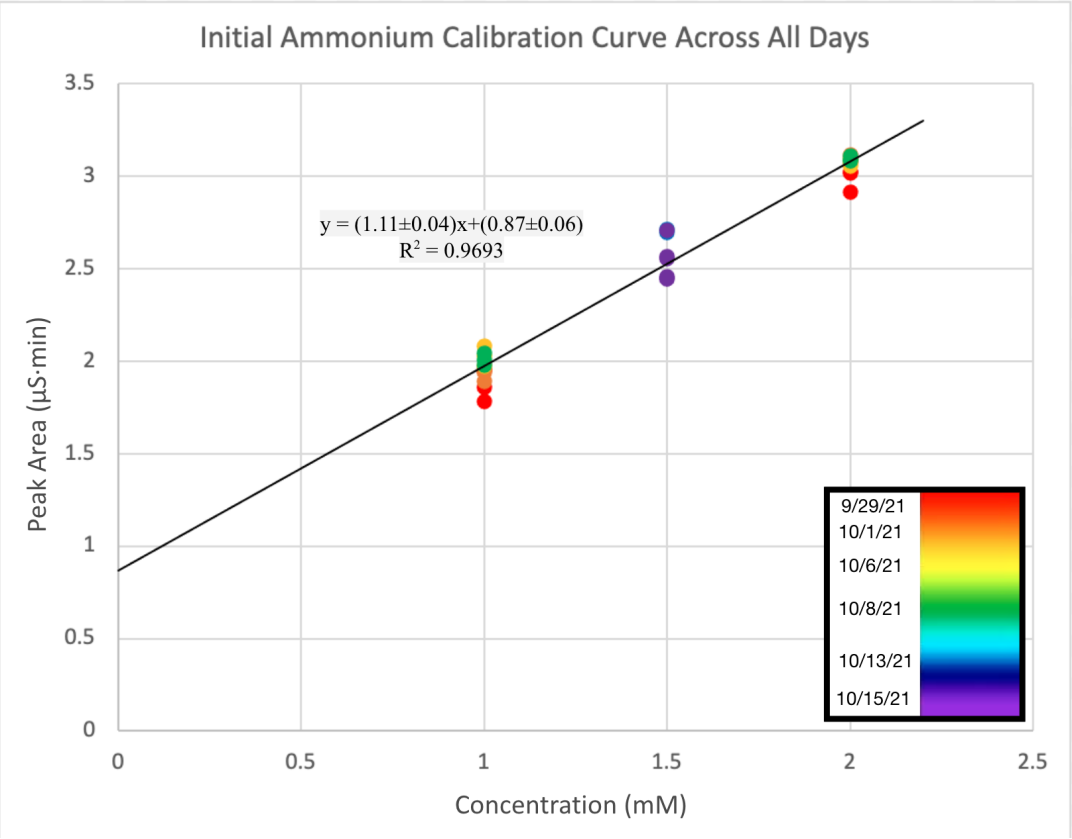

Figure 7. The initial calibration curve made for ammonium across several days. The data ranges from 1.0 mM to 2.0 mM ammonium.

Another issue encountered during these initial steps was the observation that the calibration curves made thus far had non-zero y-intercepts. The calibration curves depict the relationship between peak area and analyte concentration. For the calibration curve containing all of this initial data (shown in Figure 7), the y-intercept is 0.87 ± 0.06 µS, where the error is one standard deviation; the y-intercept is 15.4 standard deviations from zero. This same data for each individual day is shown in Figure 8. A non-zero y-intercept implies that a solution with no analyte at all still has a peak in the same location. This should not be the case, so there must be some other systematic issue. A non-zero y-intercept is common in calibration curves when the samples have a concentration high enough to saturate the detector. At high enough concentrations, the peak area reaches an asymptote due to the limitations of the detector. Around the concentrations of 1.0 and 2.0 mM, the detector is approaching saturation, so the slope of the calibration curve is less steep than it would be at lower concentrations, causing the intercept to be higher than is realistic.

Another source of a non-zero y-intercept would be improper baseline correction. If the baseline is consistently too high, then the entire calibration curve would be shifted upwards; in this scenario, the slope should be unaffected. Meanwhile, the issue of saturating the detector would have the slope be too small. The baseline for these early trials was always set at a conductivity of essentially 0 µS, because the chromatograms before the peaks were very flat. An example chromatogram of one of these early trials is shown in Figure 5. There are some deviations from 0 µS, but these are very minor. The conductivity also returns very closely to 0

μS after the peaks (around 8.5 minutes). For these trials, there was little room for debate about the baseline, so the non-zero y-intercept was not attributed to this reason.

Calibration Curve	Slope	Slope Error	y-intercept	y-intercept Error	Number of Standard Deviations y-intercept is from 0
Day 1 (9/29/21)	1.22	0.06	0.74	0.09	7.9
Day 2 (10/1/21)	1.17	0.02	0.76	0.03	22.5
Day 3 (10/6/21)	1.05	0.03	0.98	0.05	18.0
Day 4 (10/8/21	1.09	0.02	0.92	0.03	28.5
Overall	1.11	0.04	0.87	0.06	15.4

Figure 8. The slopes, y-intercepts, and errors in each for the ammonium calibration curves taken over four days as well as the overall calibration curve.

At the same time, I also began running trials containing multiple analytes; specifically, these solutions were mixtures of ammonium sulfate, potassium chloride, and sodium chloride. With more complex mixtures, the Na^+ and NH_4^+ peaks overlapped substantially, oftentimes appearing to be a single broad peak. The K^+ had a large enough retention time that it did not overlap with the other two. The overlap between Na^+ and NH_4^+ is relatively common in other experiments, because these two ions have similar selectivity for typical stationary phases. A common stationary phase, which is also what this column uses, includes carboxylate cation-exchange groups.[32,33] There are more specialty columns designed with phosphonate groups that can mitigate this issue.[32] Another solution which is more feasible is to use lower concentrations of each of these compounds. This is a result of larger concentrations yielding larger peaks, which causes them to start overlapping. Beyond the overlapping, these peaks were exhibiting tailing rather than being symmetrical. Peak tailing can also occur when analytes have a high concentration.

By making calibration standards with lower concentrations, each of these three previous issues can be minimized. Reducing these concentrations is also a reasonable choice for this specific project, because the compounds of interest should be between 0.4 mg/L and 2.0 mg/L in the atmosphere. The higher end of this range is significantly less than 1.0 mM for all the analytes of interest (for example, 2.2 mg/L is equivalent to 0.12 mM of NH_4^+, 0.096 mM of Na^+, and 0.056 mM of K^+). By using concentrations within the aforementioned range, the calibration curves become more appropriate for this project and exhibit less overlapping and tailing.

2.3. Gradient Method Development

With appropriate concentrations in each mixture, calibration curves were constructed for each of the analytes of interest. These analytes included ammonium, methylamine, ethylamine, and some inorganic cations (sodium, magnesium, and potassium ions). There was still some overlapping of the ammonium, methylamine, and sodium ion peaks; this is a fairly common problem in ion chromatography, especially when the ammonium concentrations exceeds 1 mg/L.[25,37] Additionally, the ethylamine peak was near the end of the nine-minute trial, so it would sometimes not return to the baseline when the trial ended. In such cases, any area measurements would be inaccurate and the subsequent trial may have a contaminant at an early retention time. Allowing the eluent to run for a while before running the first sample helped alleviate this issue

partially. However, it also seemed reasonable to try programming a gradient method instead of an isocratic method for the complex mixtures. An isocratic method, which is what was being used up until this point, involves the mobile phase remaining constant over the course of the entire trial. Specifically, this was 8 mM MSA in milli-Q water. A gradient method has a changing mobile phase that gradually becomes more polar. In general terms, the gradient method starts with 0.8 mM MSA and gradually increases to 8.0 mM MSA. This increases the retention time for all samples and allows them to separate better. I created five different gradient method programs that differed on how long the column was saturated with 0.8 mM MSA at the start, how slowly the transition of eluent occurred, what function the transition occurred according to, and how long the 8 mM MSA should run at the end. I decided to run 0.8 mM MSA for five minutes before adding a sample in order to fully flush the column with the starting eluent. The total trial time ranged from 15 minutes to 38 minutes; the time settled on was the full 38 minutes because this yielded the best separation when analyzing ambient samples. In terms of the function of gradient transition, the choices are linear, exponential, or logarithmic. Exponential means that the gradient transition to 8 mM MSA starts slowly and then becomes much faster. With the 38 minute trial time, the analytes start to elute around 16 minutes. With an exponential change, the eluent would be too polar at 16 minutes which would make the separation not as good as it could be. A logarithmic function starts the transition fast and it slows down towards the end. Theoretically, this should keep separation good and reduce eluting time by making the mobile phase more polar quicker. In reality, this method had very little effect. As such, a linear transition was chosen due to its simplicity. The specifications of the gradient method are as follows: 5 minutes of equilibration to 0.8 mM eluent at the start, 30 minutes ramp time, 0.24 mM/min ramp rate, and 5 minutes at 8 mM eluent at the end.

Occasionally, peaks will still have some overlap, but they are usually resolved well enough to separate with the Igor program. The two cases in which peaks are very poorly resolved is when one is much larger relative to the other and when it is the first trial of the day. For the former of these two cases, the smaller of the two peaks may appear to be a shoulder of the second when the two have similar retention times. For instance, a sample with much more methylamine than ethylamine may appear to have one large peak with a shoulder. In cases such as these, software can still usually separate the two by assuming Gaussian curves. However, sometimes the concentration difference is so pronounced and the retention times are so similar that a smaller peak is not even visible. In such cases, the one present peak is recorded as a larger area than it should be, so the calculated concentration of that species is greater than reality. It is very difficult to discern between one tall peak and two fully overlapped peaks. As such, some concentrations reported may be overestimates.[25] For the latter of the two cases in which peaks are poorly resolved, the later trials in a day tend to exhibit better separation than the earlier trials. This phenomenon is a result of the columns partially drying out when not used for a couple of days. A column that dries out has cracks introduced into the stationary phase which affects analytes' ability to diffuse between the phases. This causes peak broadening and, therefore, overlap. A small bit of air passing through a column tends to have minimal effect, so the column can be revived by running the eluent through the column. This can take some time to work, so the earlier trials often have broad peaks and poor resolution. Figure 9 shows an example of a single mixture run several times in a single day and, as the day progresses, the separation improves.

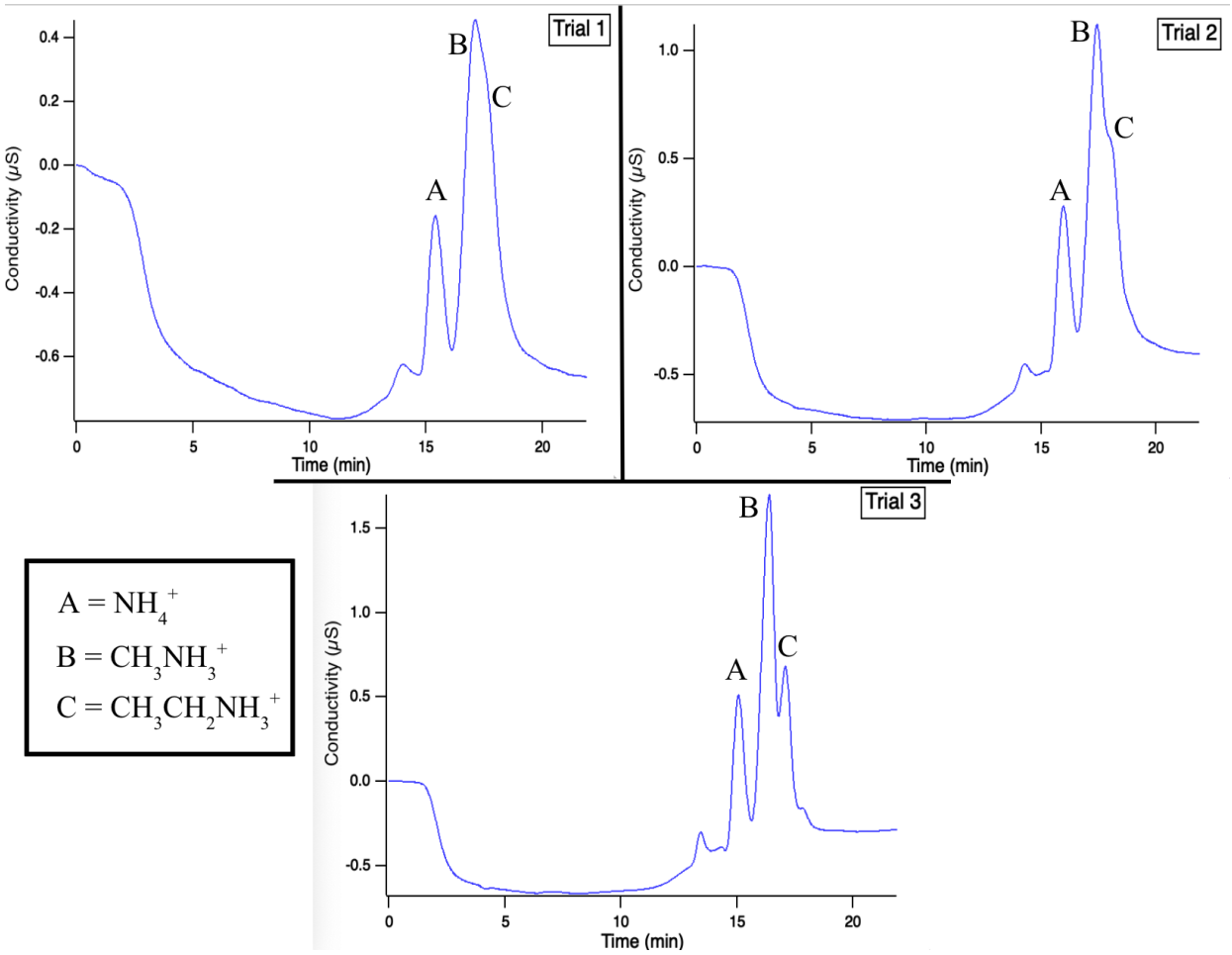

Figure 9. A mixture of 0.6 mg/L ammonium, 1.4 mg/L methylamine, and 0.6 mg/L ethylamine run through cation chromatography three times in one day. The earliest trial has the two amine peaks (B and C) substantially overlapped; the third trial has much better resolution. Igor can separate the peaks in Trials 2 and 3, but not Trial 1.

2.4. Overall Sampling Set-up

Prior to analysis with ion chromatography, samples are collected through a denuder-and-filter apparatus. The set-up is inspired by a procedure given by the Environmental Protection Agency (EPA) with some adjustments for the this specific project.[38] The apparatus — a cartoon schematic of which is shown in Figure 10 — consists of the following components attached in order: a cyclone, the first annular denuder, a filter pack, the second annular denuder, a critical orifice, and a vacuum air pump.

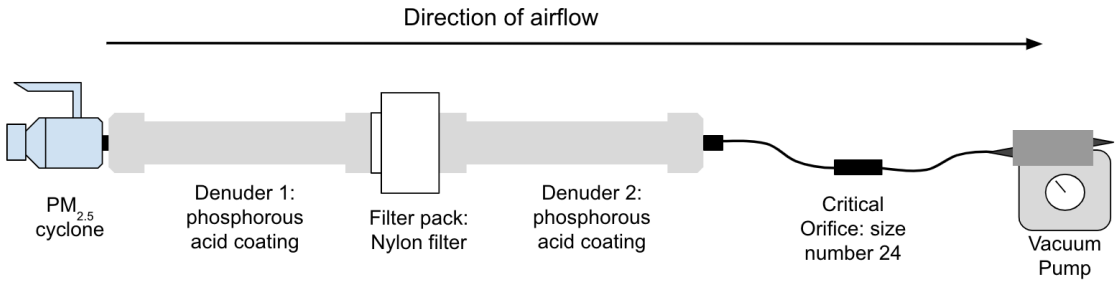

Figure 10. A cartoon schematic of the overall sampling set-up, which contains a cyclone, two annular denuders, a filter pack, a critical orifice, and a vacuum pump.

2.4.1. Cyclone

The cyclone is on one far end of the system and is the first component that air is drawn through. The air enters through the side arm of the cyclone and, through a coarse particles that have a diameter larger than 2.5 μm are pulled out of the air flow.[39] These larger particles are removed by an applied double vortex involving a centrifugal force and a fluid drag force; the inertial momentum of the spinning particles overcomes the fluid drag force for larger particles pulling them out of the air flow.[40] They are then removed into the cylindrical part of the cyclone, whereas other particulate matter and gasses continue to flow through the rest of the apparatus, since the fluid drag force overcomes the momentum.[39,40] If these larger particles were not removed, then errors could be introduced; for instance, PM_{10} contributes much more mass, thus skewing the data if collected on the filter. The cyclone used is designed for an air flow of 10 L/min, but much of the sampling was done at a much lower rate of air flow.

2.4.2. Annular Denuders

There are two annular denuders separated by a filter pack. The annular denuders are coated in a solution of 2% phosphorous acid in methanol.[25] The coating solution is added to each denuder, swirled around to coat all surfaces, and then the excess is poured out. Once coated, the denuders are dried using clean air at a flow rate of 2.8 L/min. The denuders are attached in parallel to the clean air generator using teflon tubing; after eight minutes of drying, the denuders are flipped and attached by their other opening to be dried for an additional eight minutes. The drying process is done once the glass walls have transitioned from clear to frosted in appearance.[34] As air travels through the denuders, the gasses of interest are adsorbed onto the coated walls.[34] Gasses have diffusion constants much higher than particles, so while gasses are absorbed, particles bypass the first denuder.[39] An interesting detail about denuders is that a single coated glass cylinder would need to be impractically long to have enough surface area to get adequate sample collection; as the surface area increases, the frequency of collisions between the sampled gas and the coated walls also increases. To counter this issue of low surface area, several concentric cylinders are contained within each denuder, which, increase the collisions and increase the amount of sample collected.[39]

As stated previously, some adjustments had to be made from the EPA's procedure. The first adjustment is the coating solution. The EPA procedure makes use of two different coatings: citric acid and sodium carbonate.[34] The former captures basic gasses and the latter captures acidic gasses.[34] The citric acid solution was replaced with phosphorous acid. The bond between the collected ammonia and citric acid coating is relatively weak, which causes some ammonia to flow through the system instead of being collected in the denuders; after 12 hours, up to 40% of

ammonia could exhibit desorption.[41] Alternatives are oxalic acid or phosphorous acid; both of which have negligible desorption.[25,42] Oxalic acid can displace ammonium nitrate collected on Teflon filters causing a build-up in denuders that are placed after the filter; this may be true for other filter materials as well, but this observation was made in an experiment that only utilized Teflon filters.[41] Thus, while deciding on the coating solution, oxalic acid was impractical.[41] Phosphorous acid is able to efficiently collect ammonia in the gas and particle-phases without excessive desorption, so it was chosen as the coating solution.[25,29,41] Additionally, a sodium carbonate coating was not used for the second denuder; instead, this one was also coated in 2% phosphorus acid for the purpose of collecting any particulate ammonium that vaporized off of the filter. In this project, oxidized reactive nitrogen was not being analyzed, so a sodium carbonate coating would not be useful.

The denuders are extracted by adding 5 mL of milli-Q water, washing all sides, pouring the water into a high density polyethylene (HDPE) plastic bottle, and then repeating these steps a second time.[38] This extract is left in the fume hood until analysis through ion chromatography. To prepare for IC analysis, a 10 mL Becton Dickinson Luer-Lok syringe is cleaned three times with milli-Q water and then half of the denuder extract is pulled into the syringe. A 0.22 μm syringe filter is added and around 1 mL of extract is ejected through the filter directly to waste in order to clean the filter. The rest of the extract is filtered into a clean beaker. Any remaining sample in the syringe that did not pass through the filter is sent into waste. Finally, the filtered extract is added back into the syringe.

2.4.3. Filter Pack

The filter pack is placed in between the two annular denuders. The pack is able to accommodate two filters, which were initially a Teflon filter followed by a nylon filter, in accordance with the EPA's procedure.[34] The filters are for the purpose of collecting particulate matter, the most common of which being ammonium sulfate and ammonium nitrate.[2,3] The purpose of two filters is that semi-volatile compounds that volatilize off the first can be caught by the second.[25] However, with the set-up of this experiment, the second annular denuder serves this same function. In two-filter experiments without the second denuder, this phenomenon, which is called "ammonium loss" can be quite substantial with the highest loss in one paper being 28% in the California desert in summer.[43] In this paper, ammonium loss was not measured anywhere in Colorado and was also not measured using an annular denuder after the filters. Even so, this does add an important consideration when analyzing data.[43] As for the two-filter set-up, ammonium nitrate, specifically, is poorly captured by a Teflon filter.[34] As such, for ease, most trials omitted the Teflon filter.

The nylon filter is placed in a glass bottle along with 10 mL of the IC eluent. It is then placed in an ultrasonic bath for 28 minutes. The ultrasonic bath used can run for up to eight minutes, so the bath is run for eight minutes three times and then once for four minutes. The water starts to warm up by 10 to 15 degrees after 16 minutes. At this point, the water is replaced with new cold water. The bottle is rotated 90 degrees every time the ultrasonic bath turns off, which is every eight minutes.[38] The Teflon filter, if used, is extracted using water and a small amount of absolute ethanol. The ethanol is necessary because Teflon is hydrophobic, so water alone would not get the filtered particles off of the filter paper.[44] It is then also placed in an ultrasonic bath for 28 minutes with the same procedure as the nylon filter. As stated previously, however, the Teflon filter was usually not used.

The filter extract is prepared for IC analysis using the same technique as is done for preparation of the denuder extract: a syringe is cleaned with milli-Q water, the extract is filtered through a 0.22 μm syringe, non-filtered extract is sent to waste, and the filtered extract is added back into the syringe.

2.4.4. Critical Orifice and Vacuum Pump

The critical orifice is vital for determining the total volume of air that has passed through the system over the sampling period by causing the flow rate to remain constant at its maximum possible value.[42] The critical orifice is a small metal cylinder with a hole of specific diameter (0.024 inches in this set-up). There is a pressure drop across the orifice with one side being atmospheric pressure and the other being the pressure applied by the vacuum pump.[42] Up until a point, the larger the pressure drop, the faster the volumetric flow rate of air. When the ratio of low to high pressure gets as low as 0.528, it has a sonic velocity which is the maximum; this is known as "choked flow."[42] The low pressure value can decrease without having an effect on the volume flow rate.[42] At this maximum value, the flow rate is constant, so the total volume of air sampled can be calculated using the flow rate and the total trial time.

The vacuum air pump is attached to the rest of the apparatus by plastic tubing. The pump is able to pull air through the rest of the system, and any gasses that are not collected are ejected out of one end of the pump. The pump has a pressure gauge that monitors the applied pressure on one end of the critical orifice. During all of the sampling times, the applied pressure was between 400 and 410 mbar throughout the entire sampling period.

2.5. Sampling Protocol Development

The first sample run was focused on determining if the experimental set up worked or if minor — or major — adjustments would have to be made. The largest change that was made from the initial plans to the actual sampling was the flow rate utilized. The cyclone is designed for a flow rate of 10 liters per minute (L/min) which is also the flow rate used in most of the references.[25,38] However, due to back-ordered parts, the critical orifice utilized for sonic flow of volume was a size that should cause a flow rate of 3.12 L/min instead of 10 L/min.[39] The value of 3.12 L/min was altered in a couple ways by the procedure. First, this reported value assumes an atmospheric pressure of 1 atm. However, this procedure was performed in Boulder, Colorado where the atmospheric pressure is usually lower than 1 atm. Second, the actual flow rate when measured with a volumetric flow meter showed 2.35 L/min instead, once the voltage measured was converted to flow rate. With this 2.35 L/min value, the ideal gas law was utilized to find the flow rate when operating in Boulder is 3.11 L/min.

The first sampling run was done over the course of seven days for around seven hours a day to get a total runtime of 49.5 hours. This was done because the lower flow rate causes less sample to be collected if run for the same amount of time; the sampling time must be increased to get values that are within the linear range of the calibration curves and that are greater than the limit of detection on the IC's detector. Once the sampling was complete, the two denuders, nylon filter, and Teflon filter were each extracted such that they could be analyzed.[38,44] The extract from the second denuder in the apparatus had peak areas with the right magnitude for analysis. The extract from the first denuder, however, showed a very large signal across the entire trial. This means that the concentration was too high, so it was saturating the detector. Diluting this solution in milli-Q water by a factor of 1:10 made the areas low enough to analyze. Figure 11 shows the chromatograms for the undiluted and diluted extracts of the first denuder. Figure 12 shows the

chromatograms for the second denuder, nylon filter, and teflon filter all of which were undiluted. Figure 13 summarizes the eluting times and peak areas for each trial that was collected from the 49.5 hour sampling period. Each of the filters and denuders had multiple peaks present in the corresponding chromatograms. However, the presence of peaks does not necessarily mean that the sampling procedure was successful. Before such a conclusion can be made, a blank should be analyzed for comparison and the peaks should be identified. The denuders had three peaks with retention times of approximately 18, 19, and 21 minutes. The coating solution on its own had two peaks that aligned to the first and third of the previously mentioned peaks. The middle peak, therefore, was collected during the 49.5 hours of sampling. The most likely identity of this analyte was deemed to be ammonium, since that is a reduced nitrogen species that the set-up should collect and it is the species that should have been the highest concentration (rather than amines, which should be present in lower concentrations). A sample of ammonium sulfate was run and its retention time was similar to 19 minutes, but previous work in this project has shown that retention times can fluctuate by a minute in either direction. A second test was done which was to add an ammonium sulfate spike to the denuder extract and see if a new peak appeared or if the previous one got larger. The peak did, in fact, increase in area, so it was identified as ammonium. A few samples also showed a shoulder to the ammonium peak. Using the same process as was done for ammonium, this smaller peak was identified as protonated methylamine. Methylamine was not always visible in the chromatogram; the two reasons for this are that the atmospheric concentration of methylamine was too low to be observed on most days or it overlapped with the ammonium peak which artificially makes it appear like there is more ammonium than is reality.

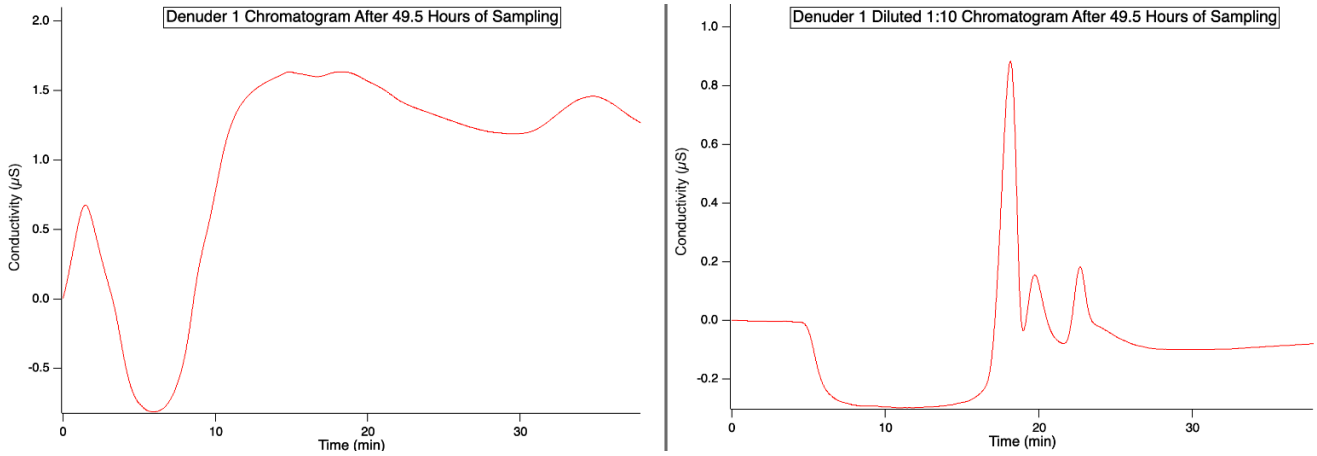

Figure 11. The chromatograms for the first denuder after sampling was done for 49.5 hours. Due to it saturating the detector, it was diluted with a ratio of 1:10; this made the peaks small enough to separate and analyze.

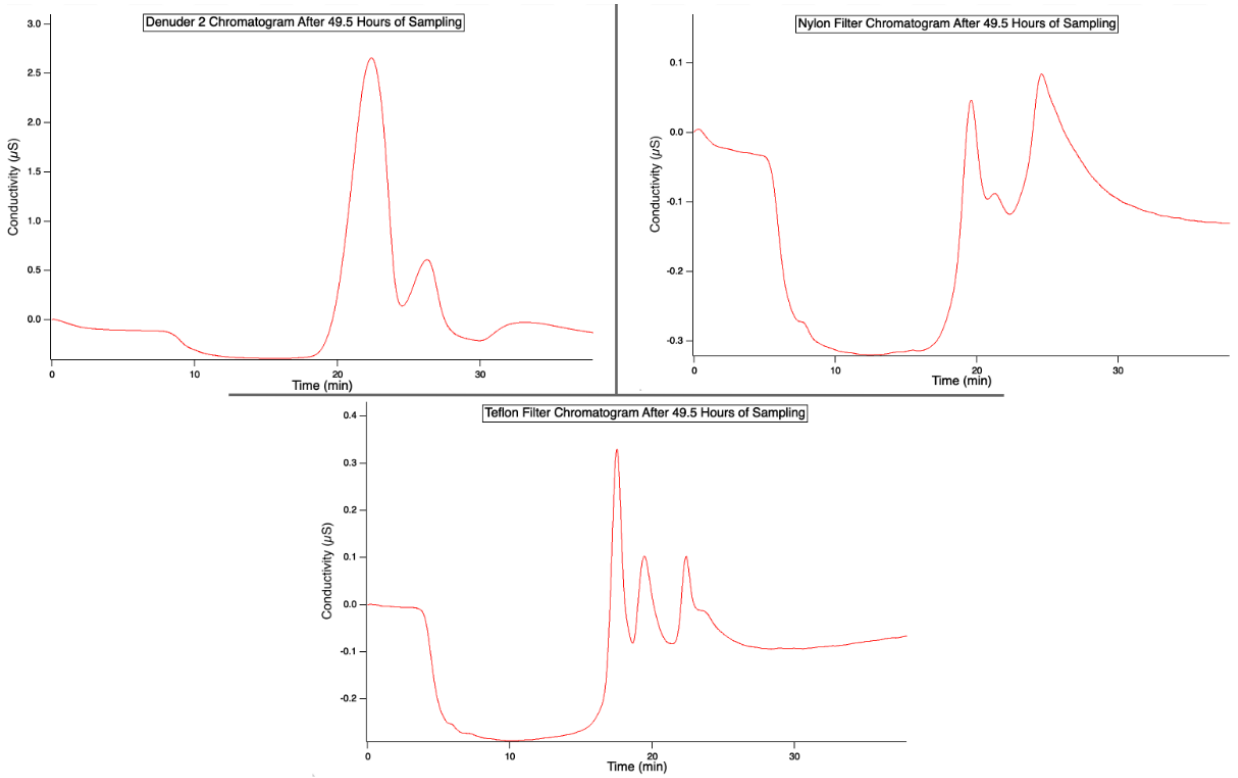

Figure 12. The chromatograms for the second denuder (top left), the nylon filter (top right), and the teflon filter (middle bottom) after sampling was done for 49.5 hours. None of these were diluted, but the second denuder has the first two peaks combined, so the individual peak areas could not be determined with Igor.

Diluted Denuder 1			Nylon Filter			Teflon Filter		
Trial	**Time (min)**	**Peak Area (µS*min)**	**Trial**	**Time (min)**	**Peak Area (µS*min)**	**Trial**	**Time (min)**	**Peak Area (µS*min)**
1	19.652	0.74962	1	19.422	0.29686	1	17.517	0.49423
	21.19	0.53567		21.182	0.22755		19.537	0.53233
	24.899	0.61744		24.706	0.65632		22.522	0.40667
2	19.372	1.1673	2	19.586	0.43664		24.466	0.13585
	21.104	0.41659		21.227	0.16307			
	24.13	0.59836		24.991	0.97354			
3	18.057	1.2899	3	20.572	0.29036			
	19.889	0.43173		22.269	0.31155			
	22.813	0.58401		25.939	0.51049			
Average	19.027	1.06894	Average	19.860	0.34129			
	20.728	0.46133		21.559	0.23406			
	23.947	0.59994		25.212	0.71345			

Figure 13. A summary of all of the eluting times and areas for the peaks in each trial that was collected from the 49.5 hour sampling period. Denuder 2 is not included, because the peaks were too broad and so they could not be analyzed (it was not diluted like the extract from Denuder 1 was).

Based on the first week of collection, it is evident that the sampling procedure works despite the smaller critical orifice. Even with a flow rate much lower than previous experimentation, 24 hours of sampling is enough to collect samples that are within the linear range of the calibration curves. Subsequent sampling periods were done for 24 hours straight, with rainy and turbulent weather being avoided. When each sampling period completes, each of the denuders and filters are kept in a fume hood until they are extracted.

The previously determined relationship between peak area and concentration for each analyte is used to determine the concentration of the sample that was run through the IC in mg/L. This concentration is multiplied by ten, which is the volume of milli-Q water or eluent used to extract the analytes (milli-Q for the denuders but eluent for the nylon filter), to get the mass of the analyte. The total mass of the analyte in micrograms is then divided by the total volume of air pulled through the pump over that particular sampling period. The total volume of air is equal to the product of the time of the run in minutes and the flow rate in liters per minute. The volume of air is also converted into cubic meters. The end value used in the long-term comparison of atmospheric concentration is in units of micrograms of compound per cubic meter of air. Uncertainties in these results derive from intrinsic error of using a calibration curve and uncertainties in the glassware used to measure solvent volume, the volume flow rate of air, and the total runtime of the sampling period. The process of calculating the concentration and error are shown in Calculation 1 and Calculation 2 in the appendix.

3. Results and Discussion

3.1. Constructing Calibration Curves

Stock solutions were made for ammonium sulfate, methylamine, ethylamine, propylamine, sodium chloride, potassium chloride, and magnesium chloride. These particular compounds were chosen due to them being analytes that could be potentially collected from the annular denuder and filter pack setup; specifically the cations of the salts (Na^+, K^+, Mg^{2+}) and the protonated versions of the amines. Na^+, K^+, and Mg^{2+} could be collected from the particle-phase and the amines could be collected from either gas or particle-phases. Each of these stock solutions were combined in various mixtures with concentrations varying from 0.2 to 2.2 mg/L, for the purpose of constructing calibration curves for each. These calibration curves depict the relationship between concentration of the analyte and the peak area on the chromatogram. However, mixtures containing all of the samples exhibited too much overlap on the chromatograms to be confident assigning the peak areas. It was for this reason that the majority of mixtures tested contained only ammonium sulfate, methylamine, and ethylamine. These three compounds are the ones that were expected to be collected in the largest amount.

Mixtures of these three compounds had concentrations varying from 0.4 mg/L to 1.8 mg/L. For ammonium, this is equivalent to 0.0222 mM to 0.0998 mM. For methylamine, this is equivalent to 0.0165 mM to 0.0580 mM. For ethylamine, this is equivalent to 0.00888 mM to 0.0399 mM. Linear relationships between peak area and concentration were found for each compound by utilizing a total of 45 trials; on a given day, a single solution would be run three times. Figure 14 summarizes the linear relationships that were derived for each of ammonium, methylamine, and ethylamine, as well as the units on the slope and y-intercept; the units for "y" are microSiemens (μS) and the units for "x" are milligrams per liter (mg/L). Other calibration curves could have been made for other inorganic cations such as sodium and potassium. Such calibration curves were not constructed, however, because they did not appear in the chromatograms for the ambient air that was sampled throughout this process. This means that the concentration of these species in ambient air is below the limit of detection for the instrument. Figure 15, Figure 16, and Figure 17 show the ammonium, methylamine, and ethylamine calibration curves respectively.

Compound	Full Calibration Curve Equation	Slope (uS*L/mg)	Error (uS*L/mg)	y-intercept (uS)	y-intercept Error (uS)
Ammonium	y = 0.61x + 0.03	0.610	0.029	0.043	0.026
Methylamine	y = 0.72x + 0.02	0.723	0.028	0.016	0.028
Ethylamine	y = 0.53x + 0.05	0.532	0.036	0.045	0.033

Figure 14. A summary of the three calibration curves that were constructed. The slopes, intercepts, and errors are reported with one digit more than significant and the full equation is reported to the appropriate number of significant figures.

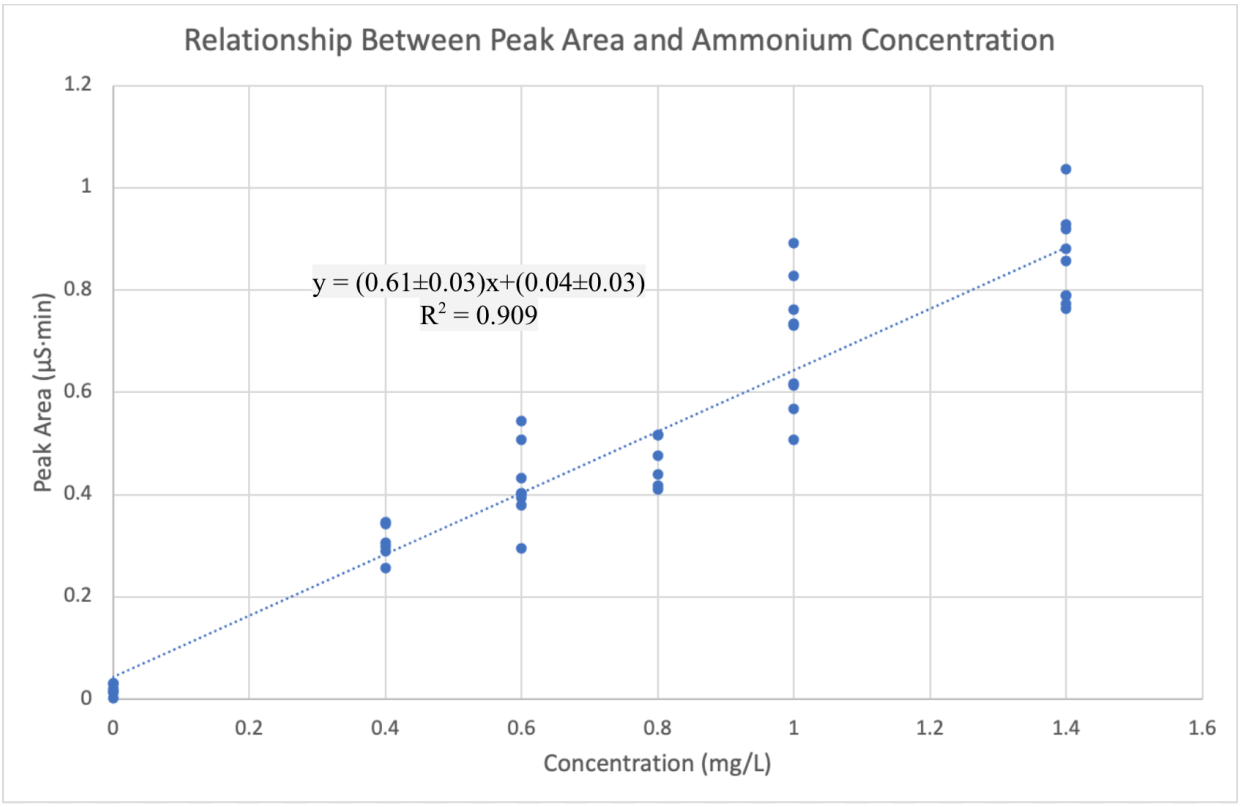

Figure 15. A calibration curve made to demonstrate the relationship between ammonium concentration and peak area of the ammonium peak from a chromatograph.

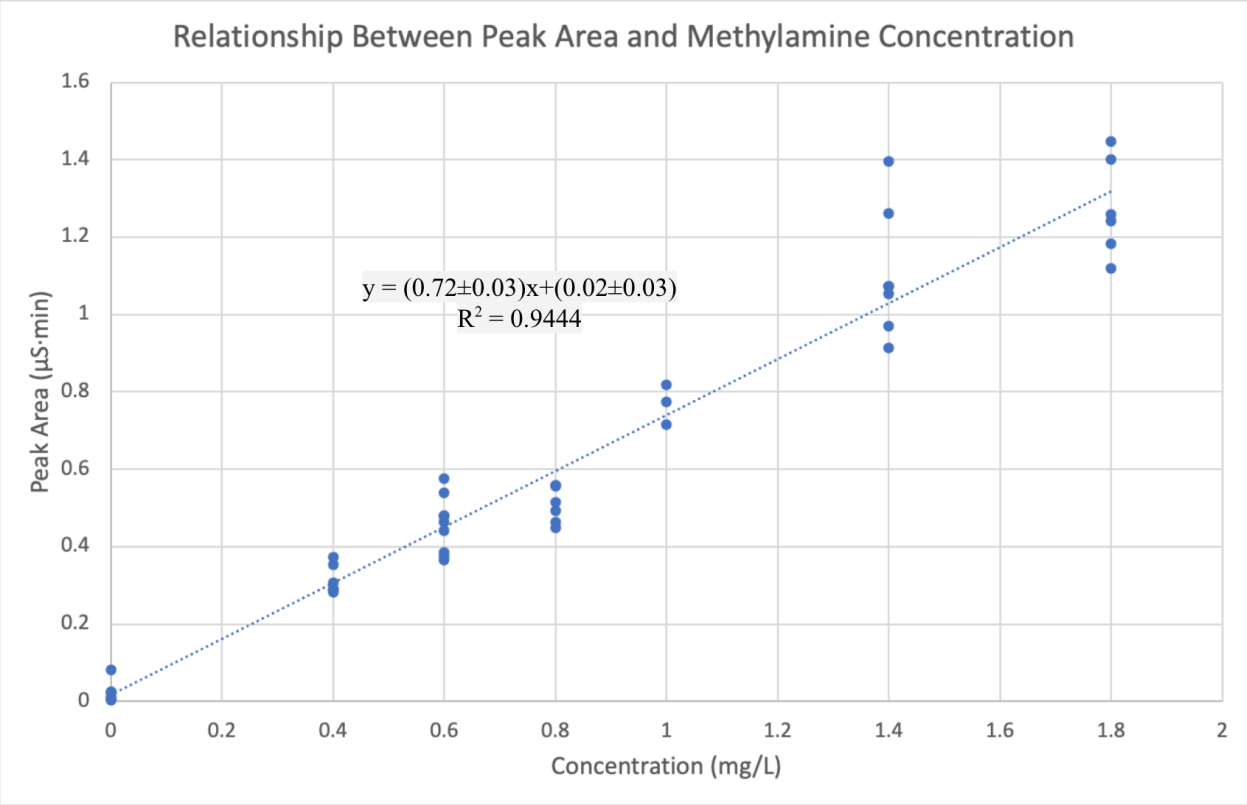

Figure 16. A calibration curve made to demonstrate the relationship between methylamine concentration and peak area of the ammonium peak from a chromatograph.

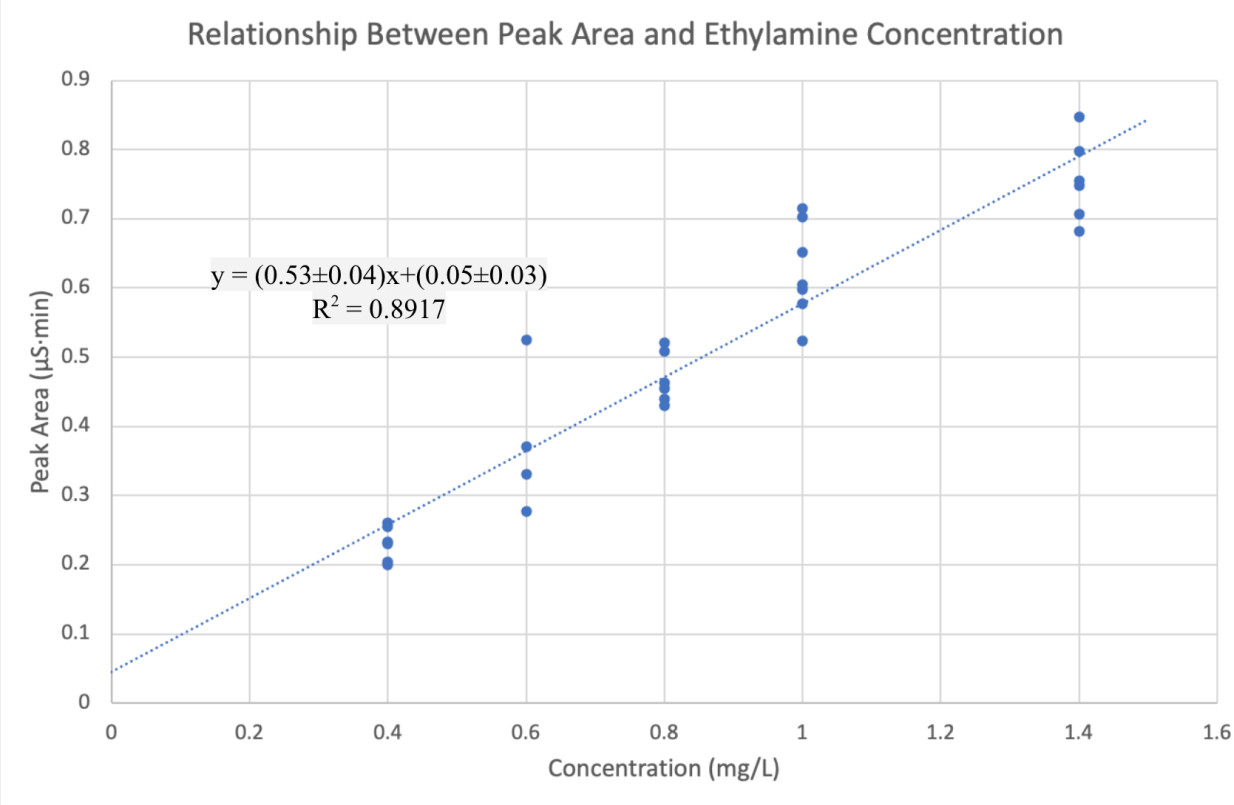

Figure 17. A calibration curve made to demonstrate the relationship between ethylamine concentration and peak area of the ammonium peak from a chromatograph.

3.2. Peak Identification

Sampling of ambient air takes place over 24 hour periods where basic species are collected from the gas and particle-phases. Following the extraction protocol described in Section 2.4.3, the resulting solutions are run through the ion chromatograph and a number of peaks appear, each one corresponding to a different compound. The chromatograms consistently had three large peaks (labeled "A," "B," and "NH_4^+"). The question that arises initially is about the identity of each of these peaks. The first step in doing so is to run some blanks of the coating solution to see if any of the three peaks are simply the coating solution rather than compounds collected from ambient air. Just the coating solution of 2% phosphorous acid in methanol has three peaks on the chromatogram; two of them correspond to peaks A and C. These could be either the result of an acid/base interaction between methanol and the phosphorous acid or an impurity in the methanol. Peaks A and B are probably from the impurities, since the set-up and sampling procedures provide a lot of time for the highly-volatile methanol to evaporate away. The initial blank that was run, shown in Figure 18, also has a peak with a retention time around 8 minutes (peak C). Peak C was only prominent in the initial blank, and is most likely the cation product of the acid/base reaction between methanol and phosphorous acid. This trial did not allow for much time for the methanol to evaporate off, which is why the peak that only appears here is identified as being due to methanol.

The second large peak that consistently appeared was identified as ammonium based on three reasons. First, the reduced N_r species expected in the largest proportion was ammonia in the gas-phase and ammonium in the aerosol phase. Second, the retention time of the peak was

similar to the retention time for ammonia in stock solutions run previously when the calibration curves were being constructed. Third, spikes of particular analytes were added to see which spikes caused a peak to increase and which caused a new peak to appear. These reasons confirm the second peak, which appeared at approximately 20 minutes, was ammonium. One example trial of the extract from the first annular denuder is shown in Figure 19.

The ammonium peak would occasionally have a shoulder which, using the same methods as before, was identified as methylamine. Figure 20 shows an example of the chromatogram of the extract from the first denuder, where a methylamine peak is visible directly after the ammonium peak. Methylamine was likely always present in the chromatogram, but only sometimes had a discernible peak from ammonium. For this reason, some ammonium concentrations determined are likely overestimates, taking into account both the ammonium and the methylamine collected. This issue exists in both the annular denuders, but lesser-so in the nylon filter. All three of these had days when the chromatograms had a visible shoulder on the ammonium peak as well as days when no-such shoulder was present.

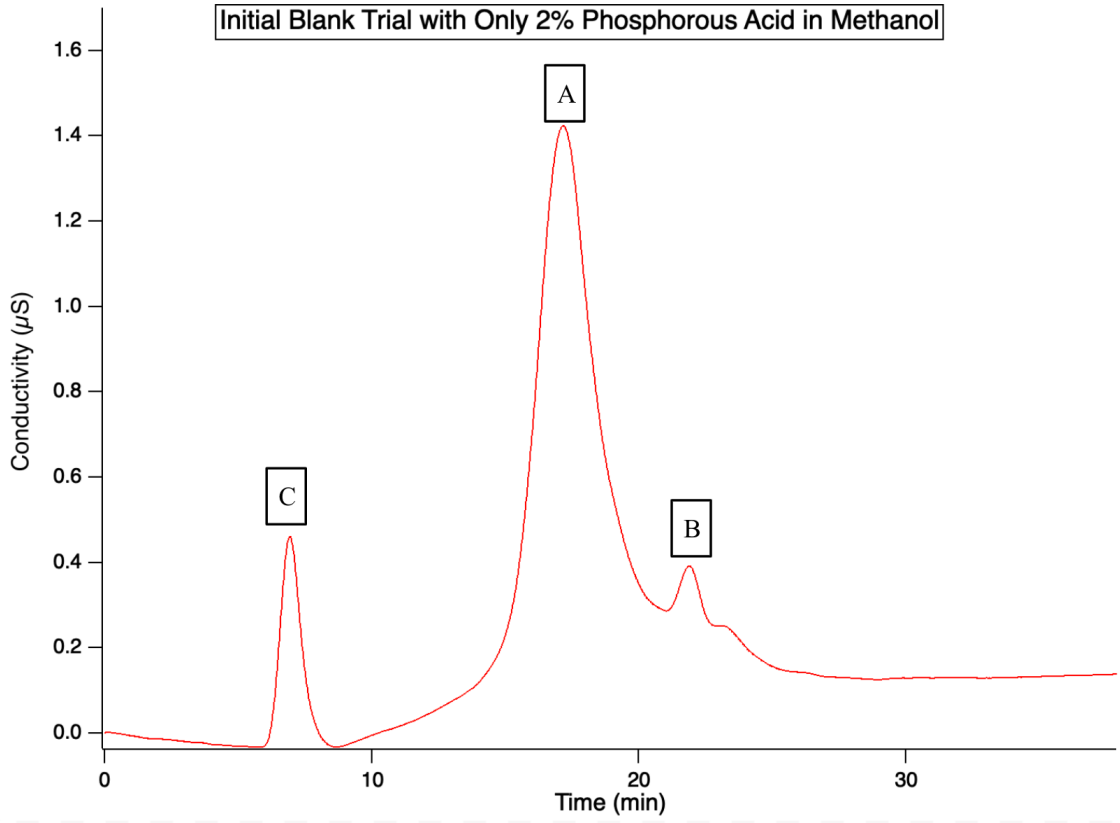

Figure 18. The initial blank that was run, which is the 2% phosphorous acid solution in methanol. This sample did not undergo the entire drying procedure or set-up process. Peaks A and B are impurities that appear consistently. Peak C only appears in this blank, suggesting it may be unevaporated methanol.

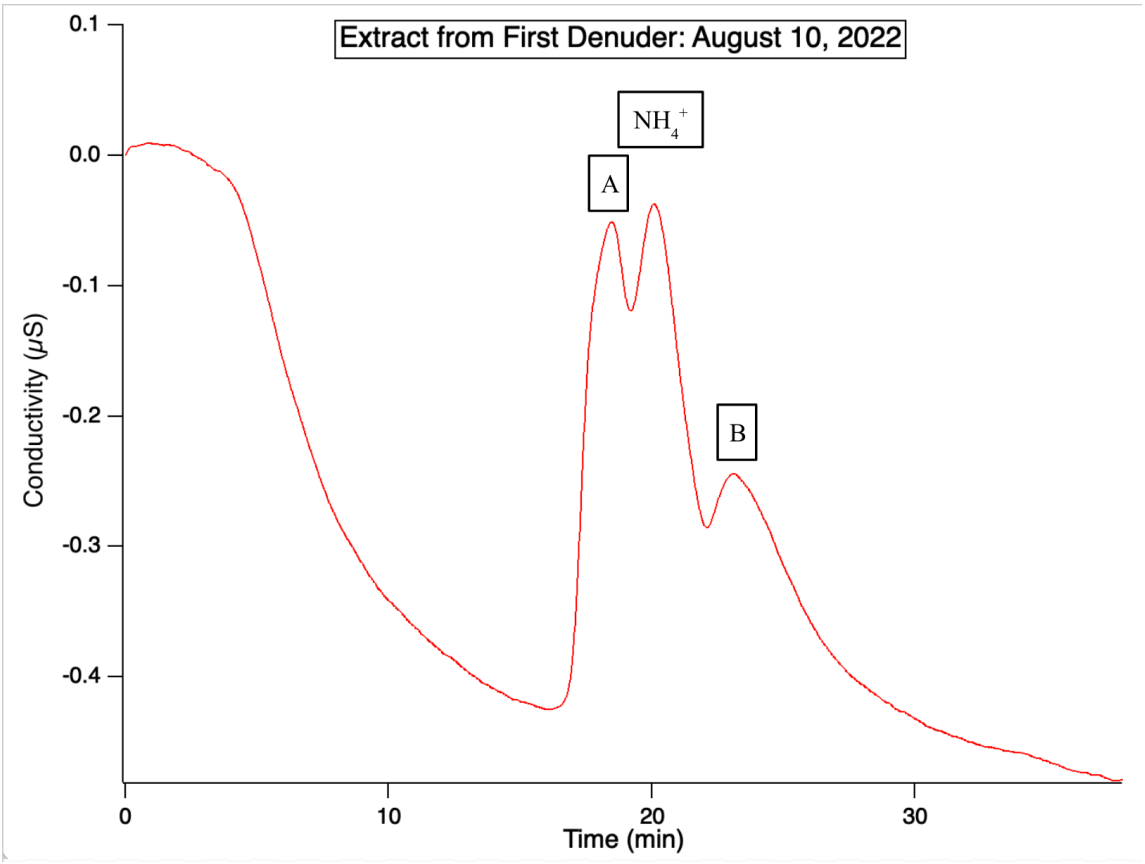

Figure 19. The chromatogram of the extract from the first denuder, for when the sampling period spanned from from August 9 to 10, 2022. Peaks A and B are impurities in the methanol; the middle peak is ammonium.

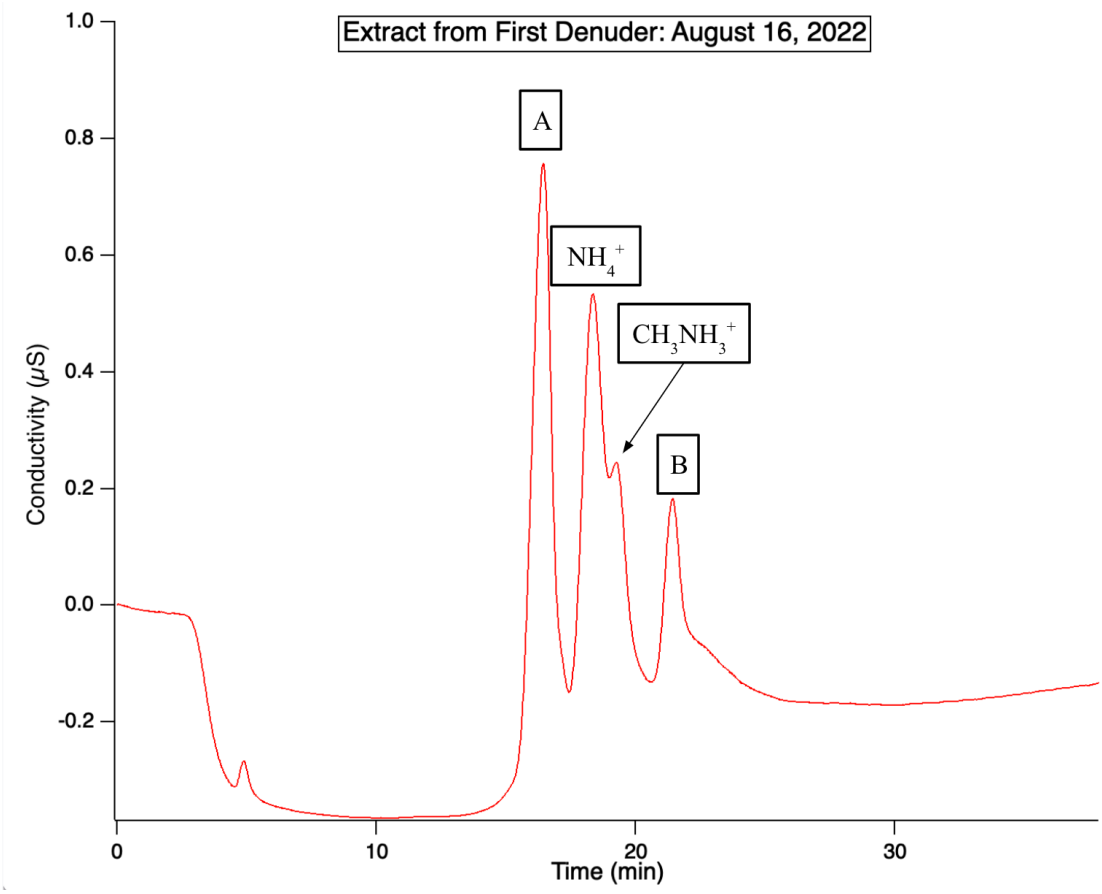

Figure 20. The chromatogram of the extract from the first denuder, where sampling was done from August 16 to 17, 2022. As in Figure 19, peaks A and B are impurities in the methanol. This chromatogram also has a new peak, which is methylamine.

The first denuder collects reduced N_r from the gas-phase, the filter collects it from the particle-phase, and the second denuder collects breakthrough and volatilized particles. None of the trials have shown evidence of methylamine on the nylon filter, but this does not necessarily mean that there is no methylamine in the particle-phase. This is a possibility, but there are a couple others as well. One option is that there is a very small concentration in the particle-phase, so it is fully enveloped in the ammonium peak. A second option is that methylamine in the particle-phase would consistently volatilize to then be caught in the second annular denuder. Whichever of these possibilities is occurring in reality helps the interpretation of the extract from the second annular denuder.

3.3. Potential Contaminants

Later, another blank was run, but this time, prior to being analyzed, the entire sample-collection process was undergone other than using the vacuum pump; the denuders were coated and dried, the apparatus was set-up and placed out of the window, and the denuders and filters were extracted. In undergoing this entire procedure, the blank that was run would also include effects of analyte collection that was not done by the pump as well as effects of the extraction procedure. The results from running these blanks were quite unusual. The first denuder had all three peaks present. The first and third (peaks A and B) are not too surprising,

since they likely derive from the coating solution. The second peak, however, provided some concerns. When the initial blanks were run and the middle peak was absent, the conclusion that was drawn is that the associated compound must be collected during the sampling procedure. With this blank, however, the pump was never turned on, so that compound should be collected in very minimal quantities. The actual concentration collected was 1.4±0.2 $\mu g/m^3$. This is smaller than the concentration usually collected with the vacuum pump. Thus, it is possible that air happened to leak through the apparatus and get collected on the denuder. The second denuder, on the other hand, had a collected concentration of 1.7±0.2$\mu g/m^3$, which is larger than the amount usually collected when the pump is turned on. The peak areas and retention times from each of these peaks are summarized in Figure 21. The conclusion that the amount collected was from a leak is now less likely given that the first denuder should collect the same as, or more than, the second denuder. The expectation that the first collects more is that the air does not have to flow as far through the system to reach the first denuder, so it would interact with more air. Besides, both denuders should collect less without the pump than with.

Two other possible explanations arise. First, in between sampling periods, the denuders are washed thoroughly with water and then left to dry in air; among other gasses, air contains NH_3, so it is possible that some traveled into the denuders while they dried. This holds true whether or not they are kept in the fume hood, because the fume hood, while containing less NH_3 from bodily emissions, does still have this gas present. In the future, this can be countered by drying the denuders using the clean air generator in the same way that is done when drying the coated denuders.

Second, there is evidence that the sample loop contains contaminants from previous trials. Milli-Q water, on its own, is usually run through the IC in between each sample. This is with the intention of cleaning out any contaminants in the sample loop or the rest of the tubing. Generally, these water trials include small peaks at the same retention times as the trial run just before. Since the peaks are present, a contaminant is as well. Furthermore, since the peaks are at the same retention times, the contaminant must be present prior to the columns; if they were present within the columns, then the peaks would appear more randomly. More recently, three water trials were performed in a row, and all three contained peaks at the retention times; each of which still contained peaks from the previous day's trials. The tubing prior to the columns contains contaminants from prior runs that take several milliliters of water to clean out. This occurrence explains why the blank from the second denuder had larger peak areas than the first: the second denuder was run afterwards and there were contaminants still present from the first denuder. Either the sample loop must be replaced or it can be cleaned with a larger volume of water in between runs. Figure 21 shows the blank that was run initially without performing the entire drying process and Figure 22 shows the blank that did include the entire sampling process (besides turning the pump on). Figure 23 gives the three water trials.

Denuder 1				Denuder 2			
Trial	Time (min)	Peak Area (µS*min)	Concentration (ug/m^3)	Trial	Time (min)	Peak Area (µS*min)	Concentration (ug/m^3)
1	17.9	0.384		1	17.4	0.405	
	19.8	0.436			19.5	0.746	
	23.6	1.013			21.6	1.043	
2	17.6	0.416		2	17.3	0.438	
	19.6	0.611			19.4	0.771	
	22.8	1.242			22.4	0.724	
3	17.2	0.463		Average	17.4	0.422	
	19.2	0.687			19.4	0.758	1.6_9 +/- 0.1_8
	22.5	1.116			22.0	0.883	
4	17.1	0.521					
	19.1	0.724					
	22.6	1.081					
Average	17.4	0.446					
	19.4	0.614	1.3_7 +/- 0.1_8				
	22.9	1.113					

Figure 21. A table summarizing the peak areas, retention times, and concentrations for the blank trials; this blank underwent the entire set-up and sampling procedure except the pump was not turned on for the sampling period of 23.25 hours. The reported error was calculated using error propagation deriving from the calibration curve, glassware, flow meter, and sampling time.

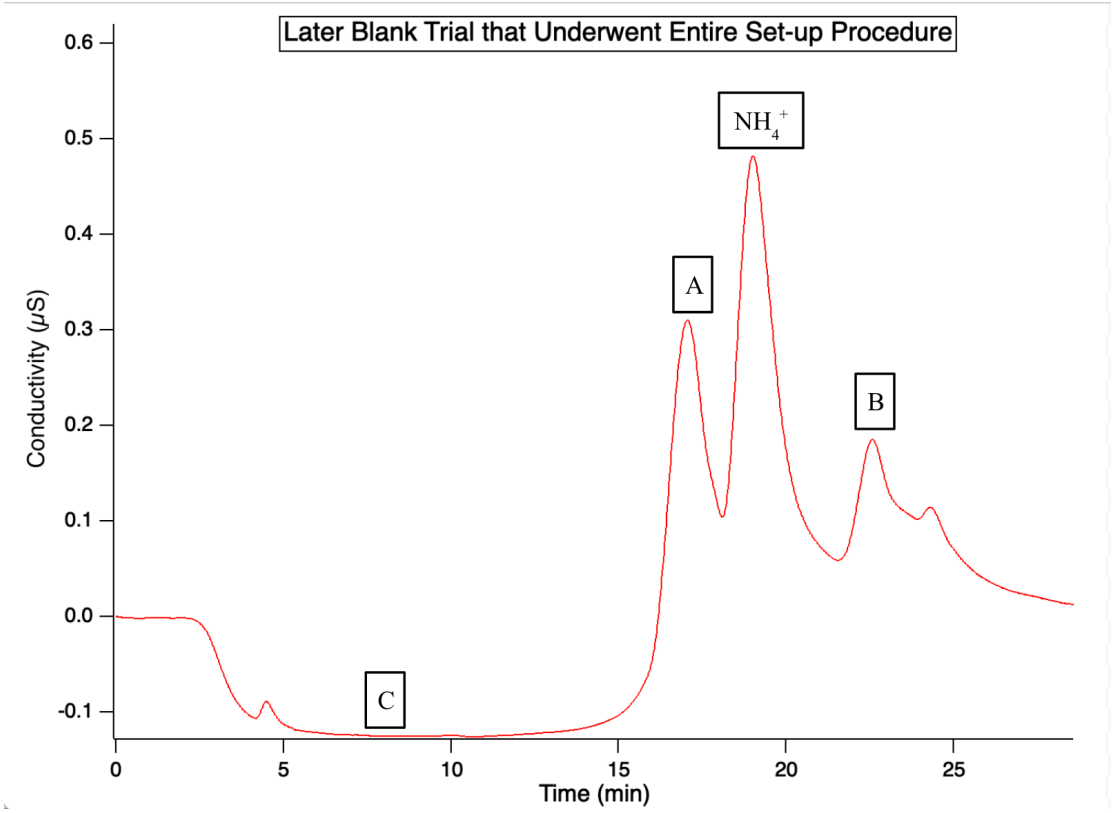

Figure 22. The later blank that was run underwent the entire set-up and sampling procedure, other than turning the vacuum pump on. Peaks A and B are impurities that appear consistently. The ammonium peak is larger than expected. The retention time of peak C, from Figure 18, is also shown even though no peak is present.

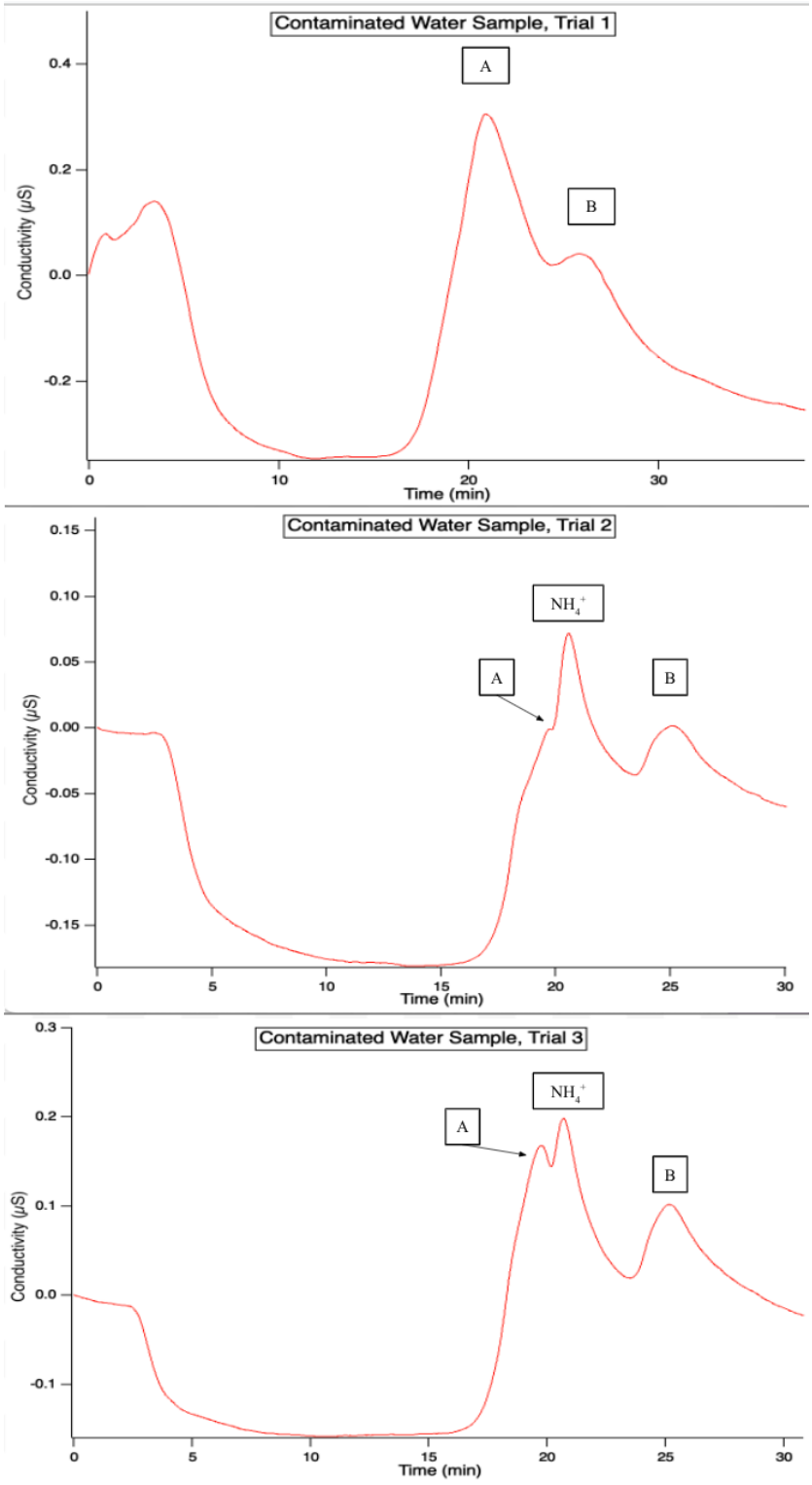

Figure 23. Three water trials with relatively large peaks, suggesting a contaminant is present from prior trials. The peaks are at consistent retention times, so the contaminant must be in the tubing before the columns.

3.4. Calculated Concentrations

As for the data collected thus far, sampling has been done for six times total where each sampling period is approximately 24 hours, starting and ending in the mid-afternoon. For each period undergone, there are three components to extract and analyze: the two denuders and the nylon filter. The retention times and peak areas for each of these were recorded using Igor and then converted into concentrations of analyte per unit volume of sampled air. A summary of these fluctuations in NH_3 over time are shown in Figure 24. Most samples did not have a visible peak for methylamine, so this fluctuation has not been plotted. As for the NH_3 changes, the first denuder always had the most NH_3 which was generally 1.3 times as much as the other two sources combined (always between 1 and 1.6 times as much).

3.5. Preliminary Trends

Since this is a long-term sampling project, it will take time for most trends to become apparent. Years-worth of data will be necessary to examine seasonal trends in gas-particle partitioning. It is also too early to make final conclusions related to trends in temperature, weather, humidity, and wind direction. Even so, the two months of sampling done thus far do allow for some preliminary analysis. For each trend, it is necessary to note that there is a lot of fluctuation on any given sampling period; with sampling done for approximately 24 hours at a time, these weather phenomena are prone to change within that period.

The first trend to consider is temperature. Most of the sampling done so far occurred in the late summer, where temperatures were generally quite high during the day. At night, these temperatures usually decrease by around 11℃ (15℉). In the gas-phase, as measured using the first annular denuder, the sampling period that had the least ammonia was August 16 to 17, 2022. This particular time, the temperature fluctuated between 15℃ and 21℃ except for the last few hours where it reached up to 27℃. Comparing this to most sampling days, the temperature was consistently significantly lower (except for the last few hours). The other sampling day that had fairly low temperatures was September 8 to 9, 2022; the temperature was 30℃ for the first 12 hours and then 15℃ for the second 12 hours. This sampling period had the most ammonia in the gas-phase, with about 1.5 times as much as the August 16 to 17 period. Due to the large fluctuation in the temperature from the first half to the second half, it is difficult to use this sampling period in trend-analysis. Two periods with high temperatures throughout the whole time were August 10 to 11 and August 29 to 30. For the former, this day had fairly low gaseous ammonia concentration. As for the August 29 to 30 period, this collection time had the second most ammonia in the gas-phase. Two other sampling periods, which were August 19 to 20 and September 1 to 2, had relatively medium temperatures that fluctuated quite a bit; they moved back and forth in the range of 18℃ to 25℃. These days also had ammonia concentrations in between the previously discussed extremes. The temperature fluctuations across these days is shown in Figure 25.

For four of these six sampling periods, there is a slight positive relationship between average temperature and ammonia in the gas-phase. This trend fails, however, for the August 10 to 11 and the September 8 to 9 sampling periods. The expected trend suggests that the former should have higher ammonia concentration and the latter should have lower than was measured.

Similar data collection was done in three urban sites of Romania in the Petrus, Popa, and Bratu paper.[45] As a point of comparison, Boulder and Romania have relatively similar daily temperatures with Boulder reaching slightly higher maxima and slightly lower minima than Romania. A larger difference is that Romania has almost 2.5 times as much annual precipitation. With that being addressed, samples were collected March to August of 2021 and they found gaseous NH_3 in ambient air to be 2.5 times as high in the summer than the spring (46.03±8.05 versus 18.62±2.92 ppb).[45] Just as I have observed, they attribute this change primarily to higher temperatures in the summer. They consider ammonia slip from catalytic converters to be an important reason for higher ammonia emissions, but other papers have found lower temperatures promote ammonia slip rather than higher temperatures.[11,45] While this may imply that summer should have lower NH_3 concentrations recorded, there are other factors affecting emissions: for instance, NH_3 emissions from animal waste increase by up to a factor of nine when temperatures vary from 5℃ to 25℃.[7] Generally, higher temperatures are expected to cause higher NH_3 emissions which, in turn, leads to higher ambient concentrations.[46]

There is still the particle-phase to consider. The two main aerosols under consideration are NH_4NO_3 and $(NH_4)_2SO_4$, each of which likely have different dependencies on temperature given their different volatility. NH_4NO_3 is semivolatile, so the expectation is that higher temperatures would favor conversion to the gas phase (NH_3), which does prove to be true in past research; similarly, past research has also shown that low humidity may favor the gas phase as well.[46,47] $(NH_4)_2SO_4$, on the other hand, is quite non-volatile, so there is less likely to be a strong preference for the gas phase when temperatures increase.

However, there is not enough evidence to confirm such a trend exists. Further sampling will be necessary for concluding the validity of this trend. Other factors exist which muddle the analysis. A simple relationship, such as the positive trend of NH_3 concentrations with temperature, assumes uniform sources and no dependence on directionality of the wind. During sampling periods, the wind direction and speed usually varied substantially over very short timeframes. Occasionally, this would be broken, such as the August 19 to 20 and September 8 to 9 sampling periods; half of each of these two periods had the normal variation while the other half had wind mostly coming from between 0° and 20°. These two periods had the most and the third most gaseous NH_3 concentration, so the source region could be another contributing factor beyond temperature. The period with the second highest concentration was August 29 to 30, which had wind directions from 270° to 280° for a quarter of the period and fluctuations for the rest. Most feedlots in Colorado, which are a large source for ammonia emissions, are between 0° and 90° from Boulder; the four closest feedlots to Boulder are between 0° and 45°. Based on the locations of these feedlots, it makes sense that days with higher ammonia concentrations recorded would be days where the wind is mostly flowing from this general direction.

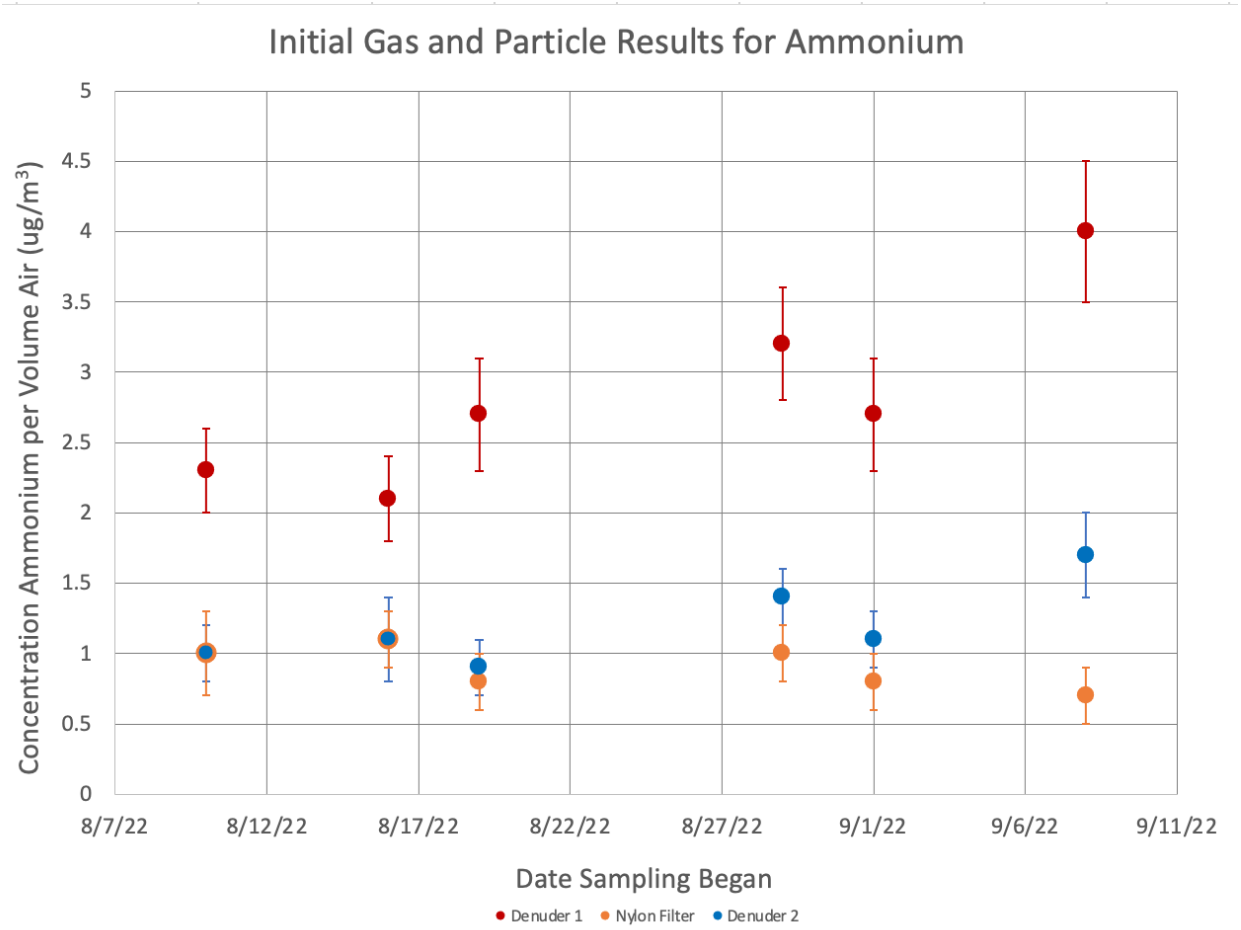

Figure 24. Concentration fluctuations for the two annular denuders and the nylon filter across sampling periods. The dates on the x-axis are when sampling began — generally in the afternoon — rather than the day sampling finished, which was the next day.

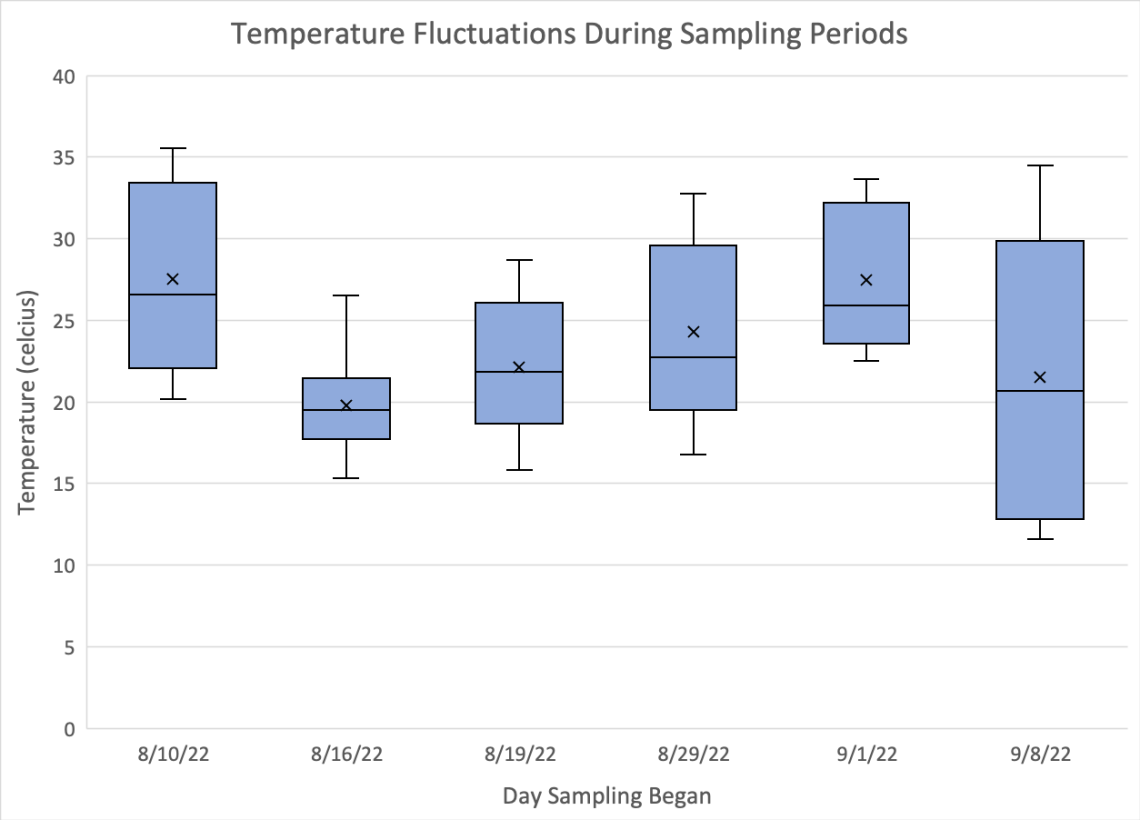

Figure 25. The temperature changes across each of the sampling periods, demonstrated in a box-and-whisker plot; the "x" is the mean, the whiskers are the maximum and minimum, the box is the upper and lower quartiles, and the horizontal line within the box is the median. The middle four fit a trend of higher temperatures corresponding to higher ammonia concentration in the gas-phase. The dates on the x-axis are given in month/day/year format.

As stated previously, the ammonia collected in the second denuder has two potential sources: gas breakthrough from the first denuder and volatilized aerosols from the filter. If we assume that the majority collected on the second denuder is from the latter of those sources, then a trend related to humidity starts to emerge. A box-and-whisker plot showing humidity changes on each of the sampling periods is shown in Figure 26. By taking the sum of ammonia collected in the second denuder and the filter, the total in the particle-phase is determined for each day (again, note that there may be peak overlap with other analytes causing overestimates or the second denuder may have collected some breakthrough). This sum seemingly had no specific trend related to temperature or humidity. The determined concentrations were 2.1 $\mu g/m^3$ with a standard deviation of 0.3 $\mu g/m^3$. If, instead, the only focus is on the ammonia collected from the nylon filter, then very similar results are found. This time, the concentrations were 0.9 $\mu g/m^3$ with a standard deviation of 0.2 $\mu g/m^3$. Once again, there seemed to be no relation to temperature or humidity.

Previously, it was discussed that NH_4NO_3 is semi-volatile, so it should transition from the particle phase at higher temperatures. The transition away from the particle phase has not yet been observed from the currently-available data set. When it comes to relative humidity, there is little consensus on the effect of humidity on gas-particle partitioning for NH_3 species. The

research in Romania, discussed earlier, found that that low humidity favored the particle phase; this paper did not specify NH_4NO_3, $(NH_4)_2SO_4$, or both.[47] Multiple other papers found low humidity favors the gas phase, specifically for NH_4NO_3; this other research did not make mention of $(NH_4)_2SO_4$.[46,48]

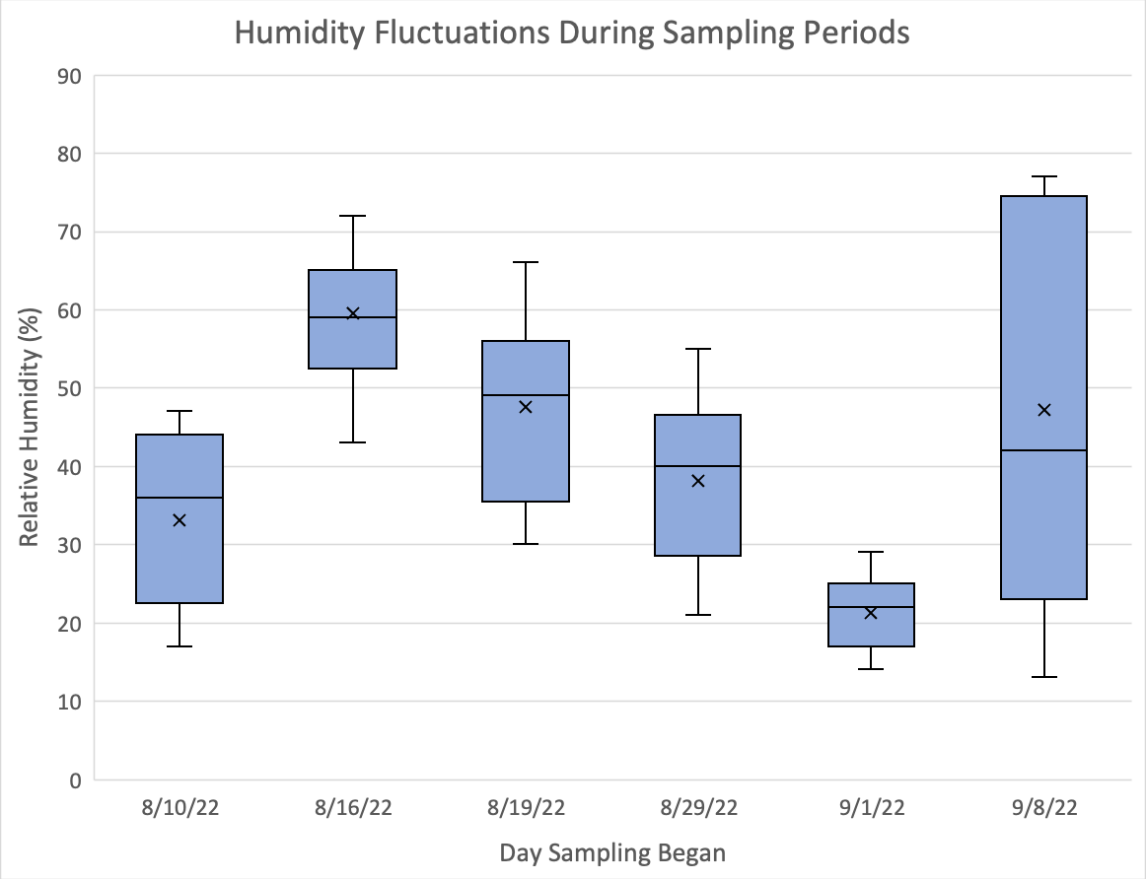

Figure 26. The humidity changes across each of the sampling periods, demonstrated in a box-and-whisker plot; the "x" is the mean, the whiskers are the maximum and minimum, the box is the upper and lower quartiles, and the horizontal line within the box is the median. The dates on the x-axis are given in month/day/year format.

The total amount of ammonia collected as well as the ratio of ammonia in the gas and particle-phases may also be affected by some weather phenomenon. Thus far, no such relationship has been noticed when looking at temperature, humidity, wind speed, and wind direction. It is also slightly too early to draw complete conclusions, because of the issues already mentioned with the second annular denuder; specifically, how much of the sample collected in it is from breakthrough versus volatilized particles.

4. Conclusion

The focus of this project was to develop a method for the long-term sampling and subsequent analysis of reduced reactive nitrogen species in the ambient atmosphere such that the seasonal and yearly trends in gas-particle partitioning can be explored. The developed method

included ambient air collection using annular denuders and a nylon filter followed by analysis through cation chromatography.[34]

Now that the procedures for each aspect of this long-term project have been created and thoroughly tested, more sampling needs to be done. This project is still in its infancy, because there are many potential results and trends that may be evident by examining a much wider array of data. When considering gas-particle partitioning of ammonia and amines, initial trends related to temperature, humidity, wind speed, and wind direction already seem plausible. With more sampling, these trends can be confirmed and further relationships may emerge, especially ones that exist on annual and seasonal timelines.

Understanding trends in this partitioning can greatly improve our ability to assess risks in fertilizer application, animal husbandry farms, biomass burning, and carbon capture and storage technology.[1,27] Reactive nitrogen (N_r) in the gas-phase often exhibits deposition near the source which can help incentivize these transgressors to attempt to decrease their emissions, since they put their own lands at risk of eutrophication, acidification, and loss of biodiversity.[4,24] Gaseous N_r can also react with sulfuric acid and nitric acid to form aerosols which can travel much farther from the source; then they can cause deposition, worsen air quality, increase risks of pulmonary disorders, and change the rate of new particle formation events hundreds of kilometers from the source of the emissions.[2,3,4,11,19] It is these far-reaching effects that demonstrate the vital importance of N_r sampling. Ammonia emissions, specifically, have a projected increase over the next century and have had limited attention in urban environments until recently.[30,31]

The general future of this project is for sampling to continue and for exploration focused on the weather effects that alter the gas-particle partitioning to continue as well. There remain some unusual and confusing results that can be examined and addressed in the near future that will improve the data collection process and improve our understanding of said data. For instance, a large concentration of ammonium was consistently collected on the second annular denuder, suggesting a large amount of particulate volatilization or excessive breakthrough from the first denuder. Another example is a common issue where ammonium and methylamine have very similar retention times and so they can overlap substantially causing an overestimate of NH_3 concentration and an apparent lack of methylamine whatsoever.[25] Perhaps refinements to the gradient method or the eventual replacement of the analytical column will allow for improved separation and more accurate data analysis.

This project in method development and refinement serves as the vital first step needed to understand the gas-particle partitioning of reduced N_r as an effect of atmospheric fluctuations and conditions. Sampling over the course of years will be necessary to obtain a full picture of the behavior of ammonia and amines, but incredible strides have been achieved by solidifying a procedure for collection and analysis.

Appendix

Ammonium Calibration Curve: $A = (0.6279 \frac{\mu S*L}{mg} * C) + 0.0560\ \mu S \rightarrow C = \frac{A - 0.0560\ \mu S}{0.6279\ \frac{\mu S*L}{mg}}$

Peak Area: $A = 0.7450\ \mu S$

Volume of Solution: $V_{sol} = 0.01\ L$

Concentration in Solution: $C_{sol} = \frac{A_{peak} - 0.0560\ \mu S}{0.6279\ \frac{\mu S*L}{mg}} = \frac{0.7450\ \mu S - 0.0560\ \mu S}{0.6279\ \frac{\mu S*L}{mg}} = 1.097\ \frac{mg}{L}$

Total Mass in Solution: $m_{sol} = C_{sol} * V_{sol} = 1.097\ \frac{mg}{L} * 0.01\ L * \frac{1000\ \mu g}{1\ mg} = 10.97\ \mu g$

Total Volume of Air Sampled: $V_{air} = 24\ hours * \frac{60\ mins}{1\ hour} * \frac{3.11\ L}{min} * \frac{1\ m^3}{1000\ L} = 4.478\ m^3$

Concentration in Air: $C_{air} = \frac{m_{sol}}{V_{air}} = \frac{10.97\ \mu g}{4.478\ m^3} = 2.450\ \frac{\mu g}{m^3}$

Calculation 1. Example determination of the concentration of ammonia in a unit volume of air.

Total Formula: $C_{air} = \frac{C_{sol} * V_{sol}}{time * flow\ rate}$

$C_{sol} = 1.097 \pm 0.105\ \frac{mg}{L}$

$V_{sol} = 0.010 \pm 0.001\ L$

$time = t = 1440 \pm 1\ min$

$flow\ rate = r = 3.11 \pm 0.0311\ \frac{L}{min}$

$$\delta C_{air} = C_{air} * \sqrt{\left(\frac{\delta C_{sol}}{C_{sol}}\right)^2 + \left(\frac{\delta V_{sol}}{V_{sol}}\right)^2 + \left(\frac{\delta t}{t}\right)^2 + \left(\frac{\delta r}{r}\right)^2} =$$

$$2.450\ \frac{\mu g}{m^3} * \sqrt{\left(\frac{0.105}{1.097}\right)^2 + \left(\frac{0.001}{0.010}\right)^2 + \left(\frac{1}{1440}\right)^2 + \left(\frac{0.0311}{3.11}\right)^2} = 0.340\ \frac{\mu g}{m^3}$$

$C_{air} = 2.5 \pm 0.3\ \frac{\mu g}{m^3}$

Calculation 2. Example utilization of error propagation to determine the uncertainty in the concentration of ammonia in a unit volume of air.

Works Cited

(1) Erisman, J. W.; Galloway, J.; Seitzinger, S.; Bleeker, A.; Butterbach-Bahl, K. Reactive Nitrogen in the Environment and Its Effect on Climate Change. Current Opinion in Environmental Sustainability 2011, 3 (5), 281–290.
(2) Li, Y.; Schichtel, B. A.; Walker, J. T.; Schwede, D. B.; Chen, X.; Lehmann, C. M.; Puchalski, M. A.; Gay, D. A.; Collett, J. L. Increasing Importance of Deposition of Reduced Nitrogen in the United States. Proceedings of the National Academy of Sciences 2016, 113 (21), 5874–5879.
(3) Nitrogen Oxides Control Regulations | Ground-Level Ozone | New England | US EPA. Https://Www3.Epa.Gov/Region1/Airquality/Nox.Html (Accessed Aug 29, 2022).
(4) Van Damme, M.; Clarisse, L.; Franco, B.; Sutton, M. A.; Erisman, J. W.; Wichink Kruit, R.; van Zanten, M.; Whitburn, S.; Hadji-Lazaro, J.; Hurtmans, D.; Clerbaux, C.; Coheur, P.-F. Global, Regional and National Trends of Atmospheric Ammonia Derived from a Decadal (2008–2018) Satellite Record. Environmental Research Letters 2021, 16 (5), 055017.
(5) Lamsal, L. N.; Duncan, B. N.; Yoshida, Y.; Krotkov, N. A.; Pickering, K. E.; Streets, D. G.; Lu, Z. U.S. No2 Trends (2005–2013): EPA Air Quality System (AQS) Data versus Improved Observations from the Ozone Monitoring Instrument (OMI). Atmospheric Environment 2015, 110, 130–143.
(6) Research and Development; Beachley, G. M.; Rogers, C. M.; Lavery, T. F.; Walker, J. T.; Puchalski, M. A. Pittsburgh, Pa, 2019; Pp 1–13.
(7) Jiang, J.; Stevenson, D. S.; Uwizeye, A.; Tempio, G.; Sutton, M. A. A Climate-Dependent Global Model of Ammonia Emissions from Chicken Farming. Biogeosciences 2021, 18 (1), 135–158.
(8) Van Damme, M.; Clarisse, L.; Whitburn, S.; Hadji-Lazaro, J.; Hurtmans, D.; Clerbaux, C.; Coheur, P.-F. Industrial and Agricultural Ammonia Point Sources Exposed. Springer Nature 2018, 564 (7734), 99–103.
(9) Bergeron, C. Aquatic Life Criteria - Ammonia. Https://Www.Epa.Gov/Wqc/Aquatic-Life-Criteria-Ammonia (Accessed Sep 26, 2022).
(10) Liu, L.; Xu, W.; Lu, X.; Zhong, B.; Guo, Y.; Lu, X.; Zhao, Y.; He, W.; Wang, S.; Zhang, X.; Liu, X.; Vitousek, P. Exploring Global Changes in Agricultural Ammonia Emissions and Their Contribution to Nitrogen Deposition since 1980. Proceedings of the National Academy of Sciences 2022, 119 (14).
(11) Farren, N. J.; Davison, J.; Rose, R. A.; Wagner, R. L.; Carslaw, D. C. Underestimated Ammonia Emissions from Road Vehicles. Environmental Science & Technology 2020, 54 (24), 15689–15697.
(12) Corder, M. EXPLAINER: Why Are Dutch Farmers Protesting over Emissions? Https://Abcnews.Go.Com/Business/WireStory/Explainer-Dutch-Farmers-Protesting-Emissions-85848026 (Accessed Oct 7, 2022).
(13) Ellis, R. A.; Jacob, D. J.; Sulprizio, M. P.; Zhang, L.; Holmes, C. D.; Schichtel, B. A.; Blett, T.; Porter, E.; Pardo, L. H.; Lynch, J. A. Present and Future Nitrogen Deposition to National Parks in the United States: Critical Load Exceedances. Atmospheric Chemistry and Physics 2013, 13 (17), 9083–9095.
(14) Particulate Matter Overview. Https://Deq.Utah.Gov/Air-Quality/Particulate-Matter-Overview (Accessed Sep 26, 2022).
(15) Central American Commission for Environment and Development: San Salvador, 2012; Pp 1–14.
(16) California Air Resources Board. Https://Ww2.Arb.ca.Gov/Resources/Inhalable-Particulate-Matter-and-Health (Accessed Oct 7, 2022).
(17) Asman, W. A.; Sutton, M. A.; Schjorring, J. K. Ammonia: Emission, Atmospheric Transport

and Deposition. New Phytologist 1998, 139 (1), 27–48.
(18) Pinder, R. W.; Gilliland, A. B.; Dennis, R. L. Environmental Impact of Atmospheric NH3 Emissions under Present and Future Conditions in the Eastern United States. Geophysical Research Letters 2008, 35 (12).
(19) Wang, S.; Nan, J.; Shi, C.; Fu, Q.; Gao, S.; Wang, D.; Cui, H.; Saiz-Lopez, A.; Zhou, B. Atmospheric Ammonia and Its Impacts on Regional Air Quality over the Megacity of Shanghai, China. Scientific Reports 2015, 5 (1).
(20) Cao, H.; Henze, D. K.; Cady-Pereira, K.; McDonald, B. C.; Harkins, C.; Sun, K.; Bowman, K. W.; Fu, T.-M.; Nawaz, M. O. Covid-19 Lockdowns Afford the First Satellite-Based Confirmation That Vehicles Are an Under-Recognized Source of Urban NH3 Pollution in Los Angeles. Environmental Science & Technology Letters 2021, 9 (1), 3–9.
(21) Galloway, J. N.; Dentener, F. J.; Capone, D. G.; Boyer, E. w; Howarth, R. W.; Seitzinger, S. P.; Asner, G. P.; Cleveland, C. C.; Green, P. A.; Holland, E. A.; Karl, D. M.; Michaels, A. F.; Porter, J. H.; Townsend, A. R.; Vorosmarty, C. J. Nitrogen Cycles: Past, Present, and Future. Biogeochemistry 2004, 70 (2), 153–226.
(22) Liu, L.; Zhang, X.; Xu, W.; Liu, X.; Lu, X.; Wei, J.; Li, Y.; Yang, Y.; Wang, Z.; Wong, A. Y. Reviewing Global Estimates of Surface Reactive Nitrogen Concentration and Deposition Using Satellite Retrievals. Atmospheric Chemistry and Physics 2020, 20 (14), 8641–8658.
(23) Porter, E.; Blett, T.; Potter, D. U.; Huber, C. Protecting Resources on Federal Lands: Implications of Critical Loads for Atmospheric Deposition of Nitrogen and Sulfur. BioScience 2005, 55 (7), 603–612.
(24) Winiwarter, W.; Amon, B.; Bodirsky, B. L.; Friege, H.; Geupel, M.; Lassaletta, L.; Raghuram, N. Focus on Reactive Nitrogen and the UN Sustainable Development Goals. Environmental Research Letters 2022, 17 (5).
(25) Sullivan, A.; Benedict, K.; Carrico, C.; Dubey, M.; Schichtel, B.; Collett, J. A Quantitative Method to Measure and Speciate Amines in Ambient Aerosol Samples. Atmosphere 2020, 11 (8), 808.
(26) Huang, S.; Song, Q.; Hu, W.; Yuan, B.; Liu, J.; Jiang, B.; Li, W.; Wu, C.; Jiang, F.; Chen, W.; Wang, X.; Shao, M. Chemical Composition and Sources of Amines in PM2.5 in an Urban Site of PRD, China. Environmental Research 2022, 212.
(27) Szulejko, J. E.; Kim, K.-H. A Review of Sampling and Pretreatment Techniques for the Collection of Airborne Amines. TrAC Trends in Analytical Chemistry 2014, 57, 118–134.
(28) Ge, X.; Wexler, A. S.; Clegg, S. L. Atmospheric Amines – Part I. A Review. Atmospheric Environment 2010, 45 (3), 524–546.
(29) Tao, Y.; Ye, X.; Jiang, S.; Yang, X.; Chen, J.; Xie, Y.; Wang, R. Effects of Amines on Particle Growth Observed in New Particle Formation Events. Journal of Geophysical Research: Atmospheres 2016, 121 (1), 324–335.
(30) Zhu, L.; Henze, D. K.; Bash, J. O.; Cady-Pereira, K. E.; Shephard, M. W.; Luo, M.; Capps, S. L. Sources and Impacts of Atmospheric NH3: Current Understanding and Frontiers for Modeling, Measurements, and Remote Sensing in North America. Current Pollution Reports 2015, 1 (2), 95–116.
(31) Nair, A. A.; Yu, F. Quantification of Atmospheric Ammonia Concentrations: A Review of Its Measurement and Modeling. Atmosphere 2020, 11 (10), 1–35.
(32) Pohl, C.; Rey, M.; Jensen, D.; Kerth, J. Determination of Sodium and Ammonium Ions in Disproportionate Concentration Ratios by Ion Chromatography. Journal of Chromatography A 1999, 850 (1-2), 239–245.
(33) Product Manual for Dionex IonPac™ CS16 and CG16 Columns; Thermo Scientific: Waltham, Ma, 2010.
(34) A Practical Guide to Ion Chromatography; Sequant Innovators in Chemical Analysis: Umeå, Sweden, 2007; Pp 3–23.
(35) Thermo Scientific Dionex Eluent Suppressors for Ion Chromatography; Thermo Scientific:

Waltham, Ma, 2010.
(36) Vanatta, L. E.; Cowles, D. C. Statistically Sound Calibration Curves for Chromatographic Methods Involving Negative Response Data. Journal of Chromatographic Science 2011, 49 (8), 610–611.
(37) Hermans, C.; Jonkers, A. C. A.; de Bokx, P. K. Determination of Amines in the Presence of Excess Ammonia by Ion Chromatography-Mass Spectrometry. Journal of Chromatographic Science 2010, 48 (7), 544–548.
(38) Research and Development; Winberry, W. T.; Ellestad, T.; Stevens, B. Midwest Research Institute: Cincinnati, OH, 1999; Pp 2–32.
(39) An Overview of URG's Manual Sampling Systems; URG Corp: Chapel Hill, NC; Pp 4–11.
(40) Clean Air Technology Center. Research Triangle Park, NC; Vol. 452, Pp 1–5.
(41) Perrino, C.; Gherardi, M. Optimization of the Coating Layer for the Measurement of Ammonia by Diffusion Denuders. Atmospheric Environment 1999, 33 (28), 4579–4587.
(42) Understanding Choked Flow of Gases; O'Keefe Controls Co: Monroe, CT, 2021; Pp 1–5.
(43) Yu, X.-Y.; Lee, T.; Ayres, B.; Kreidenweis, S. M.; Malm, W.; Collett, J. L. Loss of Fine Particle Ammonium from Denuded Nylon Filters. Atmospheric Environment 2006, 40 (25), 4797–4807.
(44) Wolfson, J. M. Determination of Microgram Quantities of Inorganic Sulfate in Atmospheric Particulates. Journal of the Air Pollution Control Association 1980, 30 (6), 688–690.
(45) Petrus, M.; Popa, C.; Bratu, A.-M. Ammonia Concentration in Ambient Air in a Peri-Urban Area Using a Laser Photoacoustic Spectroscopy Detector. Materials 2022, 15 (9), 3182.
(46) Ellis, R. A.; Murphy, J. G.; Markovic, M. Z.; VandenBoer, T. C.; Makar, P. A.; Brook, J.; Mihele, C. The Influence of Gas-Particle Partitioning and Surface-Atmosphere Exchange on Ammonia During BAQS-Met. Atmospheric Chemistry and Physics 2011, 11 (1), 133–145.
(47) Du, H.; Kong, L.; Cheng, T.; Chen, J.; Yang, X.; Zhang, R.; Han, Z.; Yan, Z.; Ma, Y. Insights into Ammonium Particle-to-Gas Conversion: Non-Sulfate Ammonium Coupling with Nitrate and Chloride. Aerosol and Air Quality Research 2010, 10 (6), 589–595.
(48) Behera, S. N.; Betha, R.; Balasubramanian, R. Insights into Chemical Coupling Among Acidic Gases, Ammonia and Secondary Inorganic Aerosols. Aerosol and Air Quality Research 2013, 13 (4), 1282–1296.